NASA TM X-1567

CALCULATIONS OF NON-DIFFUSE INFRARED RADIATION FROM THE LUNAR SURFACE INCIDENT ONTO A UNIT ELEMENT ABOVE THE SURFACE

By James K. Harrison

George C. Marshall Space Flight Center
Huntsville, Ala.

NATIONAL AERONAUTICS AND SPACE ADMINISTRATION

For sale by the Clearinghouse for Federal Scientific and Technical Information
Springfield, Virginia 22151 – CFSTI price $3.00

CALCULATIONS OF NON-DIFFUSE INFRARED RADIATION FROM THE LUNAR SURFACE INCIDENT ONTO A UNIT ELEMENT ABOVE THE SURFACE

By

James K. Harrison

George C. Marshall Space Flight Center
Huntsville, Alabama

ABSTRACT

This report presents the results of calculations of the thermal radiation from the lunar surface incident onto a flat surface of unit area located a small distance above the moon. The orientation and height of the flat surface vary. The thermal radiation from the moon's surface is assumed to be non-diffuse.

The calculations show that the thermal energy flux incident onto the flat surface can differ significantly for a lunar surface that emits radiation in a non-diffuse manner when compared to a lunar surface that emits in a diffuse manner.

TABLE OF CONTENTS

ACKNOWLEDGMENT

Wayne Griffith, Computer Sciences Corporation, did the scientific programing for this problem. Jimmy R. Watkins and Tommy C. Bannister, Space Sciences Laboratory, provided mathematical assistance.

LIST OF ILLUSTRATIONS

LIST OF ILLUSTRATIONS (Concluded)

CALCULATIONS OF NON-DIFFUSE INFRARED RADIATION FROM THE LUNAR SURFACE INCIDENT ONTO A UNIT ELEMENT ABOVE THE SURFACE

SUMMARY

The amount of infrared energy flux incident onto one side of a flat surface element of unit area located above the lunar surface has been computed. The orientation and height of the flat surface with respect to the moon's surface vary. The infrared emission from the lunar surface is not diffuse, but rather is emitted in a non-diffuse manner in accordance with a mathematical equation developed by Ashby.

The results of the calculations show that for non-diffuse infrared emission, contrary to diffuse emission, the orientation of the surface receiving the radiation and the sun position are important.

INTRODUCTION

Interest in the directional characteristics or non-diffuseness of the moon's surface infrared radiation has existed in this laboratory for several years; because of this, and to support the in-house studies, several contracts have been sponsored with outside research organizations. In one of these contracts, an empirical expression was developed by Ashby for predicting the infrared radiation emitted by the lunar surface.

In the work presented here, a sunlit area on the surface of the moon has been assumed to emit non-diffuse infrared radiation, in accordance with the Ashby expression; and the amount of this radiation incident onto one side of a flat surface element of unit area located above the moon has been calculated. The orientation and height of the element with respect to the moon's surface vary.

PURPOSE AND REVIEW OF WORK

This research program in directional infrared radiation is an attempt to partially fulfill the goal of explaining and defining the lunar thermal environment. One part of the directional radiation program is to develop a theoretical model with which one can accurately reproduce the existing experimental data and that is consistent with current knowledge of the physical structure of the moon's surface. Such a model should reveal important information about the physical features of the surface. Another part of the program is to present information about the directional aspects in a form useful to those solving problems in thermal experiments and thermal studies of the moon's surface. This report represents an effort to partially fulfill this last part. Calculations have been performed incorporating these directional effects; the results are graphically presented as infrared energy leaving the lunar surface and striking a unit area a small distance away.

To support the in-house work, a number of contracts have been sponsored with outside research organizations. In 1965 a contract with Brown Engineering Co. led to an arrangement whereby one member of the Brown research staff spent 6 months at the Boeing Scientific Research Laboratories working closely with Saari and Shorthill. These two investigators have obtained an extensive amount of data over the past 5 years on the infrared emission from the moon [1]. Their measurements have been in the 10-12 μ region of the spectrum. The purpose of the work between Brown and Boeing was to obtain from existing data a new set of measurements relating to the directional characteristics of lunar infrared emission. The effort consisted mainly of a reduction of many data points from 19 separate phases. The data were then presented graphically [2] in the form of brightness temperatures for various lunar locations and phases. A typical graph is shown in Figure 1.

Using the experimental results from the foregoing work and working under the sponsorship of Space Sciences Laboratory, Ashby and Burkhard have developed an expression for predicting the infrared emission that takes into account the directional behavior of the radiation [3]; comparisons with experimental data show it to be reasonably accurate. The chief drawback of the formula is that it has an empirical rather than a theoretical derivation and, therefore, does not give any information about the physical characteristics of the lunar surface.

When the work was first begun, the only experimental infrared data that had been examined (to the author's knowledge) for any directional characteristics were those of Pettit and Nicholson [4] and Sinton [5], and these data showed only a slight deviation from a Lambertian surface emission. It has been known for some time that sunlight is reflected by the moon's surface in a strongly directional manner. Although this is in a different part of the spectrum from the infrared, it did help to stimulate an initial interest in taking a closer look at the directional aspects of the infrared emission. The Pettit, Nicholson, and Sinton data and the photometric data were the basis for the speculation that the emission might be directional to a significant degree and deserved further investigation.

The lunar landing of Surveyor I in 1966 led to the conclusion that a pronounced directional emission did exist. The explanation of the temperature values recorded on the faces of the two instrument compartments of Surveyors I and III [6, 7] required this directionality, and subsequent investigations of earth-based measurements by Saari and Shorthill [8] reaffirmed this.

Some of the Saari and Shorthill data showing the directional aspects are presented in Figure 2. Measured results from earth-based telescopes are compared with calculated results using the previously mentioned Ashby expression. For each elevation angle of the sun, the brightness temperature is shown (for a diffuse surface the brightness temperature is a single point and is shown as an open circle). By comparing the diffuse value with the non-diffuse points, the degree of directionality can be ascertained. Notice that the radiation exhibits the greatest non-diffuseness, i.e., directionality for small sun elevation angles. Another point to notice is that the largest temperature values occur, for each sun elevation angle, when the surface is viewed from the sun direction: that is when an observer views the surface with the sun behind him. This means that a greater part of the infrared radiation is emitted toward the source, i.e., the sun, than in any other direction. Such behavior may be referred to as back-emitted, a term analogous to backscatter for the reflected sunlight from the moon that is reflected or scattered more toward the source than in any other direction.

Gross surface roughness has been suggested as the reason for the back-emitted directional radiation. This thought was put forth by Pettit and Nicholson to explain their measurements of non-diffuse radiation, and still appears to be the most satisfactory explanation. The surface, if assumed to consist of peaks and valleys (or of numerous craters and rocks), will receive sunlight mainly on the side facing the sun. The other side will be in the shadow and will, therefore,

be at a much lower temperature. This condition will exist to the greatest degree when the sun is near the horizon, and to the least degree (or not at all) when the sun is straight overhead.

The earth-based measurements were made with telescopes that have resolutions of the order of 8 - 10 seconds of arc. At the lunar distance, this means that the measurements average the radiation (at the moon's center) over a circular region of approximately 14 - 18 km in diameter. Whether the measurements would reveal this same directional characteristic over a much smaller region, say on the order of a few meters, is an unanswered question. The surface would probably be more diffuse. The reason given earlier — gross surface roughness — would not suffice to explain any directional behavior observed on this scale.

THERMAL EMISSION PER UNIT SOLID ANGLE

The emission of infrared energy from a local area on the moon in a given direction can be computed from Lambert's equation, $I(\epsilon) = I_0 \cos \epsilon$, if the emission is assumed to be diffuse. However, if the emission is non-diffuse, as recent data indicate [7], the infrared emission from a local area on the moon in a given direction can be more accurately determined from the following expression, which was developed under a NASA contract [3].

$$I_0(i, \epsilon, \alpha) = \frac{a_1 \cos i + a_2 \cos \alpha'}{1 + a_4 \dfrac{\sin \alpha'}{\cos i}} + \frac{a_3}{\pi} [(\pi - |\alpha|) \cos |\alpha| + \sin |\alpha|] \qquad (1)$$

where:

$$\alpha' = \frac{\pi}{2} \sqrt{\frac{i^2 + \epsilon^2 - 2i\epsilon \cos(\phi_i - \phi_\epsilon)}{\frac{\pi^2}{4} + \frac{4i^2\epsilon^2}{\pi^2} - 2i\epsilon \cos(\phi_i - \phi_\epsilon)}}$$

$I_0(i, \epsilon, \alpha)$ = Infrared radiance in watts/m^2 - steradian

$a_1 = 335.417$

$a_2 = 97.626$

$a_3 = 51.603$

$a_4 = 84.377$

(All of the a's are empirically determined using the Saari and Shorthill data of references 1 and 2, and have units of watts/m^2 - steradian.)

$i, \epsilon, \phi_i, \phi_\epsilon, \alpha$ = Angles defined in Figure 3.

This expression holds true only for a sunlit surface; therefore, it is not useful during the lunar night or for lunar areas that are completely in shadow. From equation (1) the infrared energy is

$$I(i, \epsilon, \alpha) = I_0(i, \epsilon, \alpha) \cos \epsilon \tag{2}$$

The brightness temperature of a local lunar area when observed from different directions and for different sun elevation angles can be obtained from equation (1) as follows:

$$T_B = \left[\frac{\pi I_0(i, \epsilon, \alpha)}{\sigma} \right]^{\frac{1}{4}} \tag{3}$$

where:

σ = Stefan-Boltzmann constant (5.673×10^{-8} watts/m^2 - °K^4)

The brightness temperatures as obtained from equation (3) for two sun elevation angles are shown in Figure 4.

TOTAL THERMAL EMISSION

If the infrared emission in the direction of dA_2 from many local areas, such as dA_1 (Fig. 3), is summed over a local lunar surface area A_1, the energy incident onto dA_2 can be determined. The energy from dA_1 to dA_2 is found by using equation (4) below. The angles ϵ and θ are required to compensate for

the skewness of the surfaces with respect to each other, while the term r^2 represents the attenuation of the energy in accordance with the inverse square law.

$$dE = \frac{I_0(i, \epsilon, \alpha) \cos\epsilon \cos\theta}{r^2} dA_1 dA_2 \tag{4}$$

where:

dE is the energy flux from dA_1 to dA_2 in watts

The lunar area A_1 is taken as flat and circular with a radius R. Summing over A_1 and assuming dA_2 to be unity gives

$$E = \int_{A_1} \frac{I_0(i, \epsilon, \alpha) \cos\epsilon \cos\theta}{r^2} dA_1 \tag{5}$$

where:

E is the energy flux from A_1 to dA_2 in watts/m^2

Formulating r and dA_1 in terms of the fundamental angles gives

$$dA_1 = \bar{h}^2 \tan\epsilon \sec^2\epsilon \, d\phi \, d\epsilon \tag{6}$$

$$r = \bar{h} \sec\epsilon \tag{7}$$

Substituting equations (6) and (7) back into equation (5) gives

$$E = \int_0^{\tan^{-1} R/\bar{h}} \int_0^{2\pi} I_0(i, \epsilon, \alpha) \cos\theta \sin\epsilon \, d\phi \, d\epsilon \tag{8}$$

The angle θ can be obtained for any orientation of dA_2 and in terms of ϵ, γ, and ϕ by

$$\theta = \cos^{-1} [\cos\epsilon \cos\gamma - \sin\epsilon \cos(180 - \phi) \sin\gamma], \quad \theta < \pi/2$$
$$\theta = \pi/2 \qquad , \quad \theta \geq \pi/2 \tag{9}$$

Because of the limits of integration, the integration over ϕ is done in four parts — one part for each quadrant of A_1. Finally,

$$
\begin{aligned}
E = & \int_0^{\tan^{-1} R/\bar{h}} \int_0^{\phi^{**}} I_0(i, \epsilon, \alpha) \cos\theta \sin\epsilon \, d\phi \, d\epsilon \\
& + \int_0^{\tan^{-1} R/\bar{h}} \int_{\pi/2}^{\pi - \phi^{*}} I_0(i, \epsilon, \alpha) \cos\theta \sin\epsilon \, d\phi \, d\epsilon \\
& + \int_0^{\tan^{-1} R/\bar{h}} \int_{\pi + \phi^{*}}^{3\pi/2} I_0(i, \epsilon, \alpha) \cos\theta \sin\epsilon \, d\phi \, d\epsilon \\
& + \int_0^{\tan^{-1} R/\bar{h}} \int_{3\pi/2 + \phi^{***}}^{2\pi} I_0(i, \epsilon, \alpha) \cos\theta \sin\epsilon \, d\phi \, d\epsilon
\end{aligned}
\tag{10}
$$

The values for ϕ^{*}, ϕ^{**}, and ϕ^{***} depend on the orientation of dA_2. The values and corresponding orientations are as follows:

$$
\begin{aligned}
\phi^{*} &= 0 && ; \quad \gamma < \pi/2, \; 0 < \epsilon \leq |\gamma - 90| \\
\phi^{*} &= \cos^{-1}\left(\frac{\tan|\gamma - 90|}{\tan\epsilon}\right) && ; \quad \gamma < \pi/2, \; |\gamma - 90| < \epsilon \leq \tan^{-1} R/\bar{h} \\
\phi^{*} &= \pi/2 && ; \quad \gamma \geq \pi/2
\end{aligned}
$$

$$
\begin{aligned}
\phi^{**} &= \pi/2 && ; \quad \gamma \leq \pi/2 \\
\phi^{**} &= \cos^{-1}\left(\frac{\tan|\gamma - 90|}{\tan\epsilon}\right) && ; \quad \gamma > \pi/2, \; |\gamma - 90| < \epsilon \\
\phi^{**} &= 0 && ; \quad \gamma > \pi/2, \; |\gamma - 90| \geq \epsilon
\end{aligned}
$$

$$
\begin{aligned}
\phi^{***} &= 0 && ; \quad \gamma \leq \pi/2 \\
\phi^{***} &= \sin^{-1}\left(\frac{\tan|\gamma - 90|}{\tan\epsilon}\right) && ; \quad \gamma > \pi/2, \; |\gamma - 90| \leq \epsilon \leq \tan^{-1} R/\bar{h} \\
\phi^{***} &= \pi/2 && ; \quad \gamma > \pi/2
\end{aligned}
$$

RESULTS OF COMPUTATIONS

Equation (10) has been integrated numerically. Figure 3 provides an explanation of the angles involved in the integration, and Figure 5 is helpful in understanding the results. Figures 6 - 17 present the results of the computations using equation (10). Shown on each figure is the infrared energy flux from an area A_1 of the lunar surface (assumed to have an infrared emittance of unity) incident onto one side only of the element A_2 for different sun elevations. Each curve represents a different tilt angle γ for A_2. Each group of figures (four to a group) represents a single azimuthal orientation ϕ_2, of the element. When ϕ_2 is 180°, the element faces west. These curves are intended to have usefulness primarily for purposes of thermal design.

It is instructive to delineate as plainly as possible the directional aspects. One way of doing this is by comparing a diffuse and non-diffuse case for one orientation of the element, as is done in Figure 13. As in the previous figures, energy is plotted against sun position. A better way of showing the directional characteristics is by normalizing the energy values in Figures 6 - 12 about the maximum value (the curve for $R/\bar{h} = 1000$, $\gamma = 0$) for each azimuthal orientation, ϕ_2, of the element. This normalized result or view factor is more useful for performing thermal radiation calculations. Figures 14 - 20 show the view factor presented as in the previous graphs. The difference in the figures, as before for the energy curves, is the azimuthal orientation of the element and the ratio of size of the lunar surface to the height above the surface of the element. Figure 14 is typical of the other figures and will be used to point out some of the significant points. In Figure 14 the element always points west, i.e., $\phi_2 = 180°$. As the sun moves from the sunrise to sunset position, the directional aspects of the radiation can be plainly seen on comparison with the diffuse value, which is shown as a single point (although it could be shown as a horizontal line through this point). Notice particularly the general shape of the curves, how the energy striking the element is greatest near sunrise, i.e., when the sun elevation angle is small and decreases as the sun moves from this position through lunar noon, finally having the smallest view factor when the sun is near sunset and facing the element. For an element facing east ($\phi_2 = 0°$), the shape of the curve is exactly reversed, i.e., the smallest view factor occurs at sunrise and the greatest occurs at sunset. The other figures are for elements facing in other directions. Notice the element facing north ($\phi_2 = 90$), Figure 20. The curves are almost flat, meaning that almost no changes in the surface radiation occur for changing sun angle when the lunar surface is observed from such a direction. This is somewhat evident

from Figure 4 where the shape of the model indicates the distribution of the energy. Notice that the radiation is asymmetrically in the plane containing the surface normal and the east-west axis (the plane containing the sun vector) and symmetrical in the plane containing the surface normal and the north-south axis.

The curves shown in Figures 14 - 20 are for an element confined to one quadrant of the azimuthal plane, i.e., $\phi_2 = 90° - 180°$. For elements facing directions other than this, symmetrical considerations depicted in Figure 4 can be used to get the view factor from the values shown here. For example, the view factor values are the same for $\phi_2 = 225°$ as for $\phi_2 = 135°$. Figure 4 aids in understanding why this is so since the figure shows that the brightness temperature or energy in these two directions is the same. For $\phi_2 = 45°$, the values are the same as for $\phi_2 = 135°$, but the abscissa on the graph must be reversed, i.e., the scale should begin with 180° and end with 0°. When this is done, the view factor values that were at 30° sun elevation (for example) will appear instead at 150° sun elevation. This reversing scheme must always be used when the element faces between $\phi_2 = 0° - 90°$ or $270° - 360°$.

The curves clearly show the effects of the back-emitted radiation since the largest view factor occurs when the element faces away from the sun.

This variation of energy with element position can be shown in another way by having the element rotate about an axis vertical to the moon's surface (i.e., rotation in the azimuthal plane) while the sun's position is fixed. This is shown in Figure 21. The element itself is vertical to the surface ($\gamma = 90°$) and the diffuse values are again shown as a single point. Notice that the radiation shows no change when the sun is straight overhead ($\omega = 90°$). This is because the radiation is symmetrical with respect to the azimuthal plane. This trend toward symmetry in the azimuthal plane as the sun approaches lunar noon can be observed in Figures 2 and 4. Infrared measurements of the full moon, such as those of Pettit and Nicholson, are for this condition; and directional aspects when viewed from earth are at a minimum.

FINAL REMARKS

One method for taking the directional aspects of the lunar surface infrared radiation into account in numerical calculations has been shown. The results presented here have shown that calculations based on diffuse radiation may be as much as 80 W/m^2 (16 percent of total) at variance with calculations

based on non-diffuse radiation (Fig. 13). Orientation of the surface receiving the radiation and sun position are also important. For a sun elevation angle of 30°, the radiation striking a surface which is oriented vertically to the lunar surface may vary as much as 120 W/m^2 (33 percent of total) as the surface is rotated 180° about a vertical axis (Fig. 21).

George C. Marshall Space Flight Center
National Aeronautics and Space Administration
Huntsville, Alabama, December 22, 1967
129-04-02-00-62

REFERENCES

1. Saari, J. M., and Shorthill, R. W.: Isothermal and Isophotic Atlas of the Moon, NASA CR-855, September 1967.

2. Montgomery, C. G.; Saari, J. M.; Shorthill, R. W.; and Six, N. F., Jr.: Directional Characteristics of Lunar Thermal Emission. Brown Engineering Company, Inc., Technical Note R-213; Also Published as Boeing Document D1-83-0568, November 1966.

3. Ashby, Neil, and Burkhard, D. G.: Study of Radiative Aspects of Lunar Materials. Final Report on Contract NAS8-20385, Covering Period April 26, 1966 to January 26, 1967. P. E. C. Research Associates, Inc.

4. Pettit, Edison, and Nicholson, Seth B.: Lunar Radiation and Temperatures. Astrophys. J., vol. 71, 1930, p. 102.

5. Sinton, W. M.: "Temperatures on the Lunar Surface," Physics and Astronomy of the Moon, ed. Z. Kopal. Academic Press, 1962, p. 411.

6. Lucas, J. W., et al.: "Lunar Surface Thermal Characteristics." Chapter IV, Surveyor I Mission Report, Part II: Scientific Data and Results. Technical Report No. 32-1023, Jet Propulsion Laboratory, California Institute of Technology, Pasadena, Calif., 1966. Also published in J. Geo. Res., vol. 72, no. 2, pp. 779-789, January 15, 1967.

7. Lucas, J. W., et al.: "Lunar Surface Temperatures and Thermal Characteristics," Surveyor III Mission Report, Part II: Scientific Results. Technical Report 32-1177, Jet Propulsion Laboratory, California Institute of Technology, Pasadena, Calif., June 1, 1967.

8. Saari, J. M., and Shorthill, R. W.: "Review of Lunar Infrared Observations," vol. 13, Physics of the Moon, ed. S. Fred Singer, AAS Science and Technology Series, 1967.

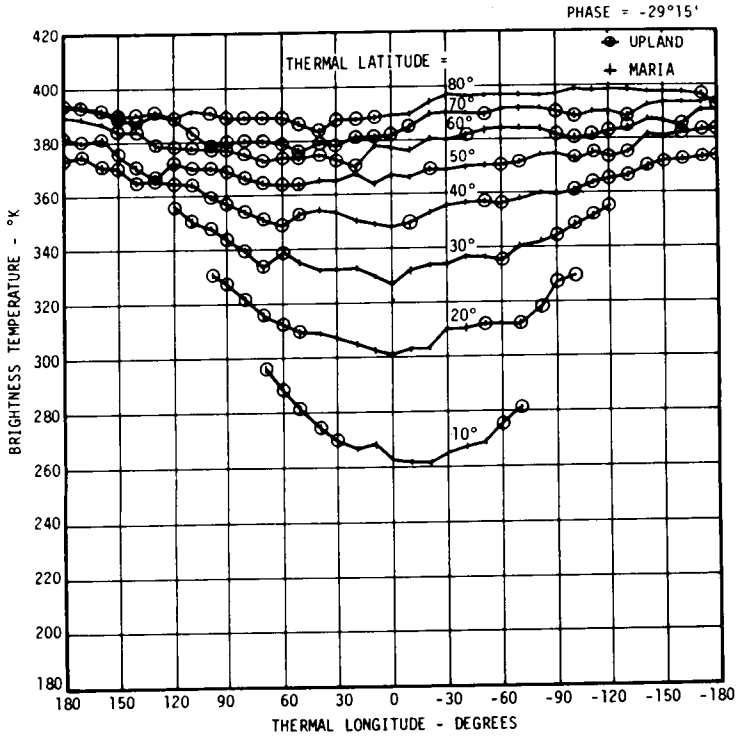

(a) Brightness Temperature Versus Thermal Longitude at Phase -29° 15'

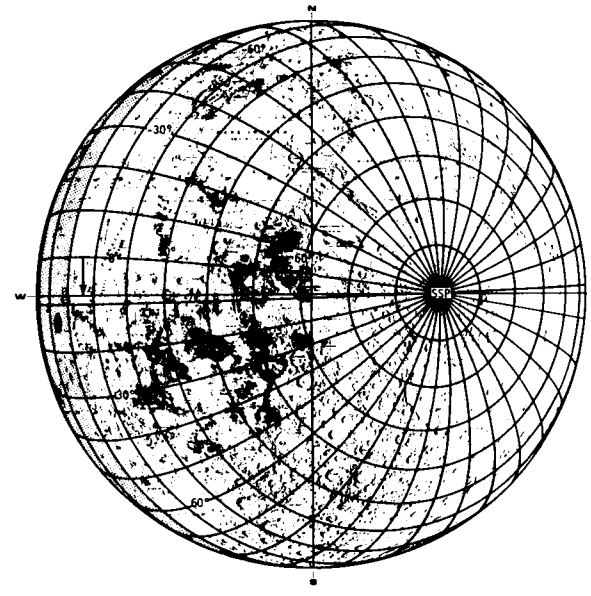

(b) Thermal Coordinate Grid for Phase Angle -29° 15'

FIGURE 1. LUNAR BRIGHTNESS TEMPERATURE FOR A SINGLE PHASE AND VARIOUS LUNAR LOCATIONS

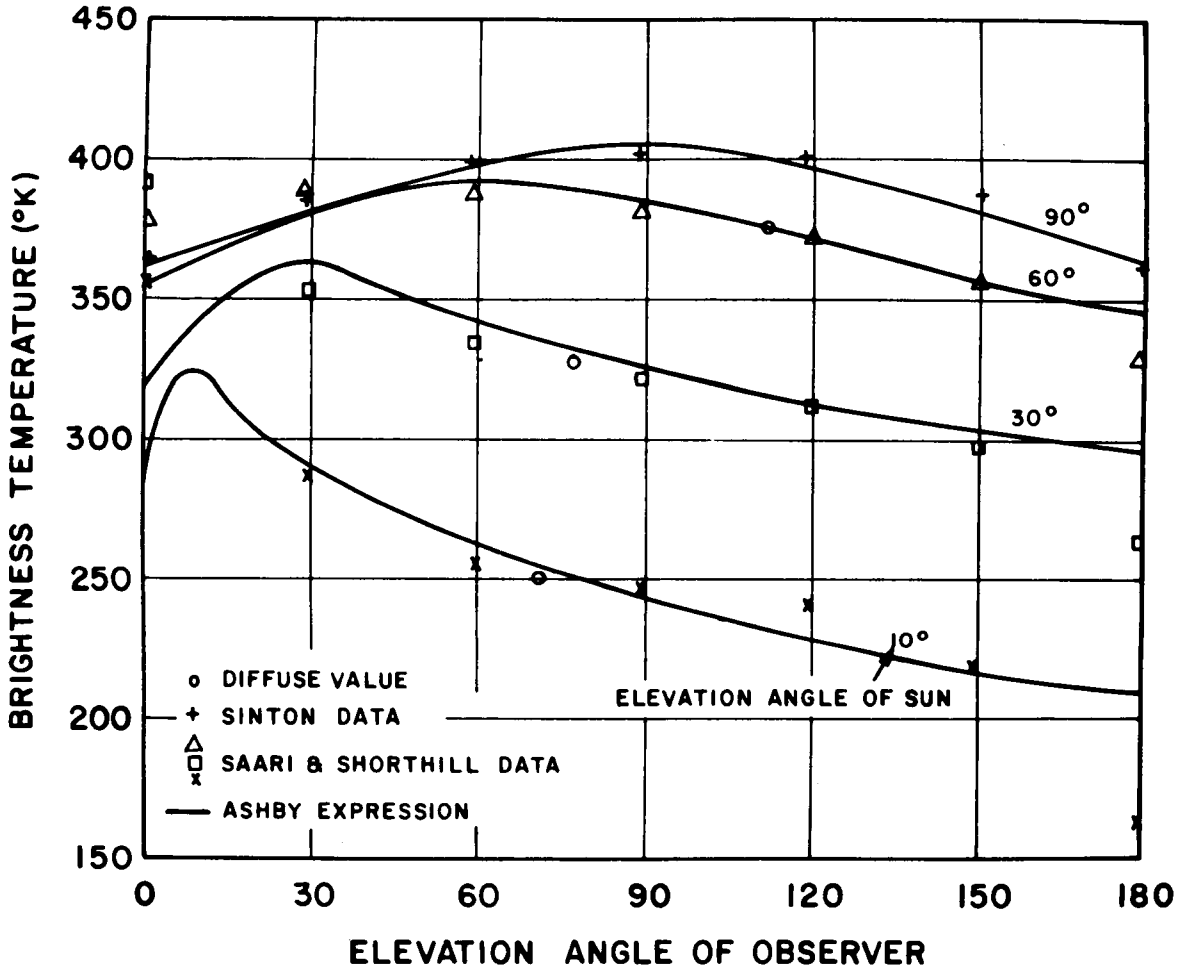

FIGURE 2. LUNAR BRIGHTNESS TEMPERATURE AS A FUNCTION OF THE ANGLE OF OBSERVATION FOR SEVERAL ELEVATION ANGLES OF THE SUN
(The elevation angles are measured from the lunar surface in the direction of sunrise and in the plane containing the sun vector and the normal to the lunar surface.)

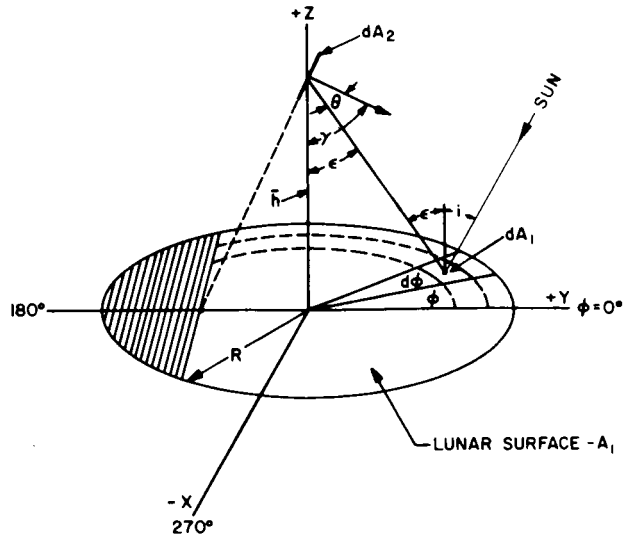

(a) Angles Involved in Integration of Equation (10)

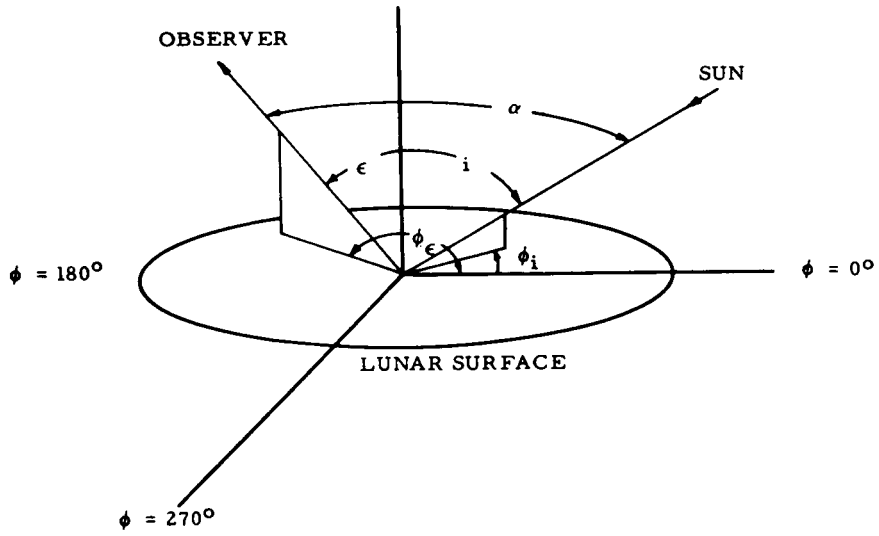

(b) Angles Used in Equation (1)

FIGURE 3. ANGLES INVOLVED IN DISCUSSION AND CALCULATIONS

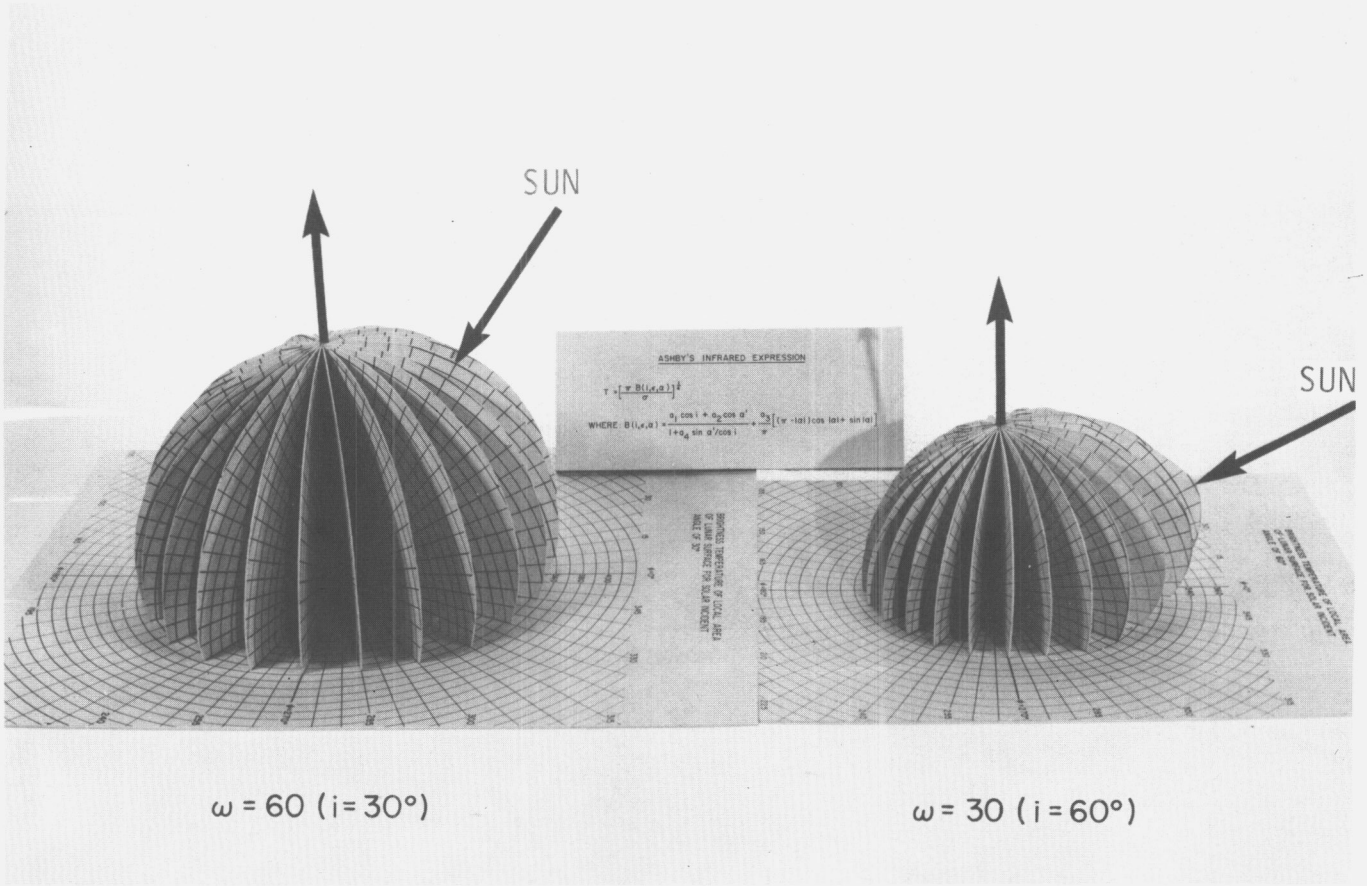

(a) $\omega = 60°$ (i = 30°) (b) $\omega = 30°$ (i = 60°)

FIGURE 4. BRIGHTNESS TEMPERATURES FOR SUN ANGLES OF 30° AND 60° MEASURED FROM THE SURFACE NORMAL (The size of the models indicates the magnitude of the temperatures)

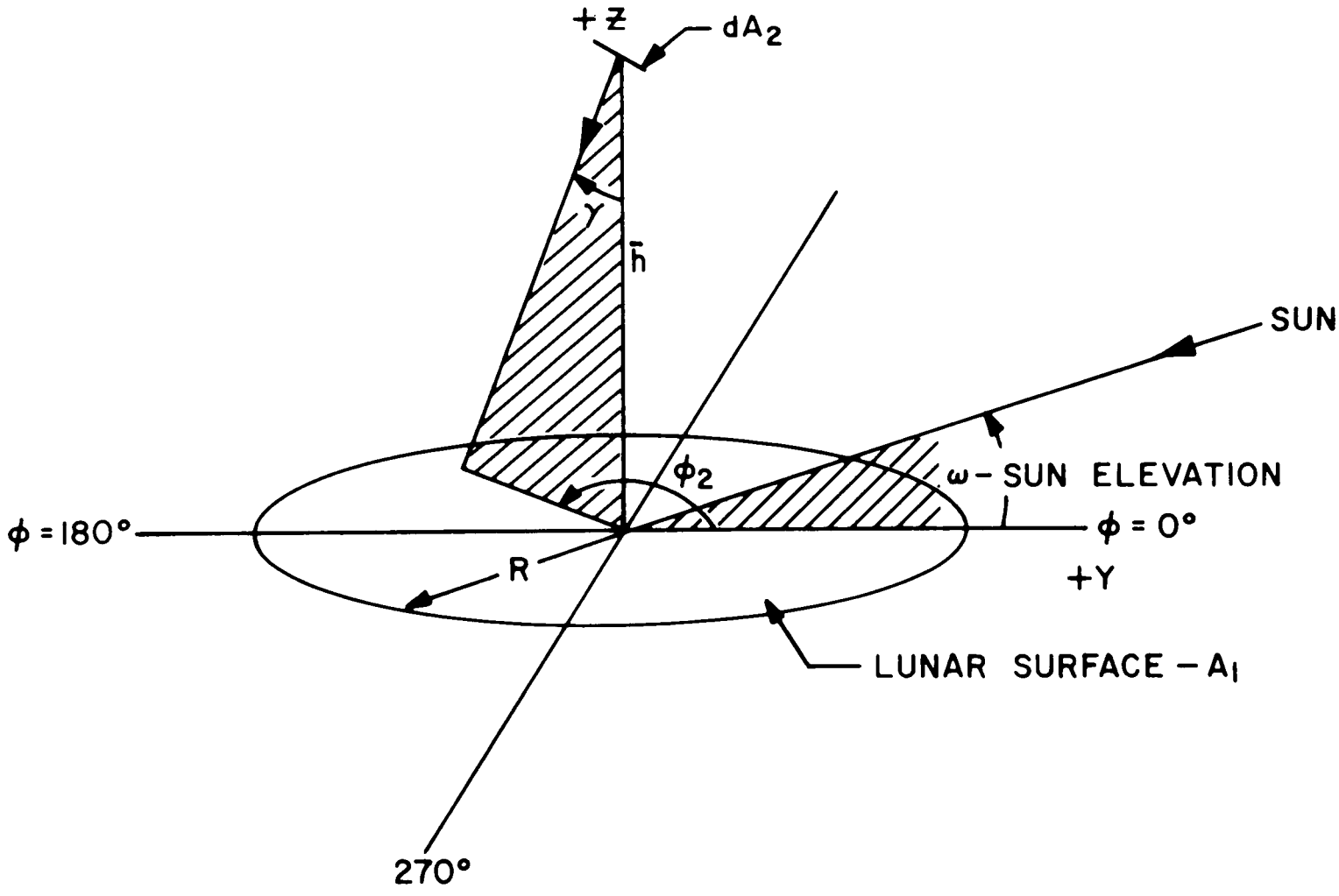

FIGURE 5. ANGLES USED IN CALCULATIONS OF FINAL RESULTS

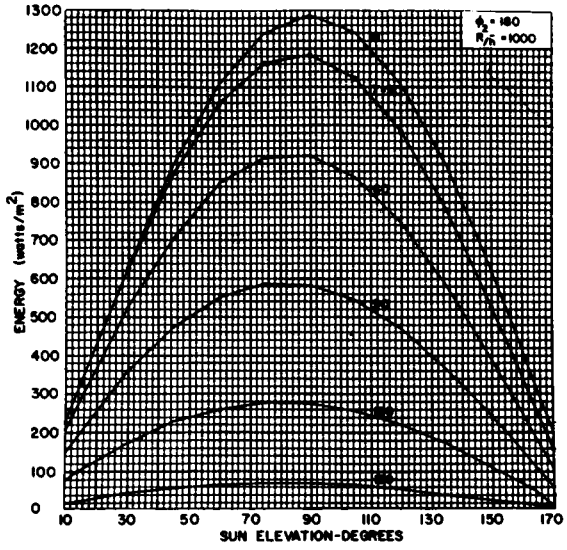

(a) $\phi_2 = 180°$, $R/\bar{h} = 1000$

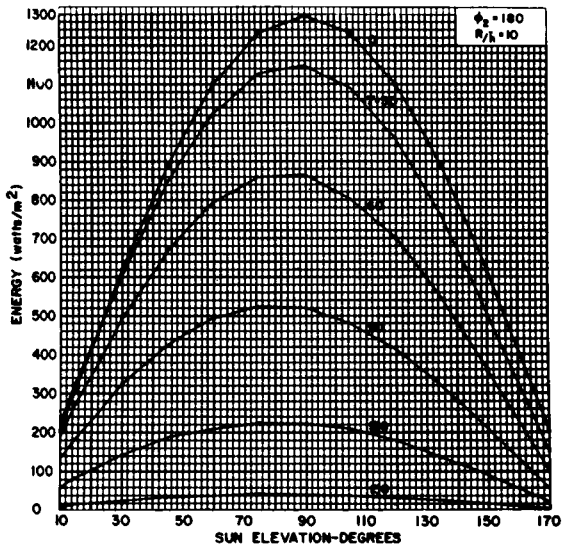

(b) $\phi_2 = 180°$, $R/\bar{h} = 10$

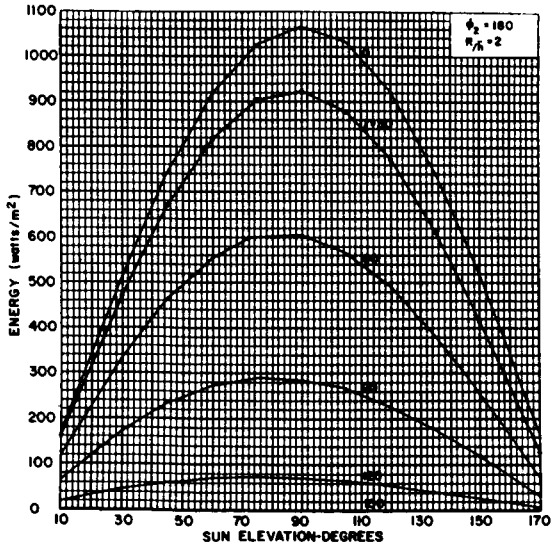

(c) $\phi_2 = 180°$, $R/\bar{h} = 2$

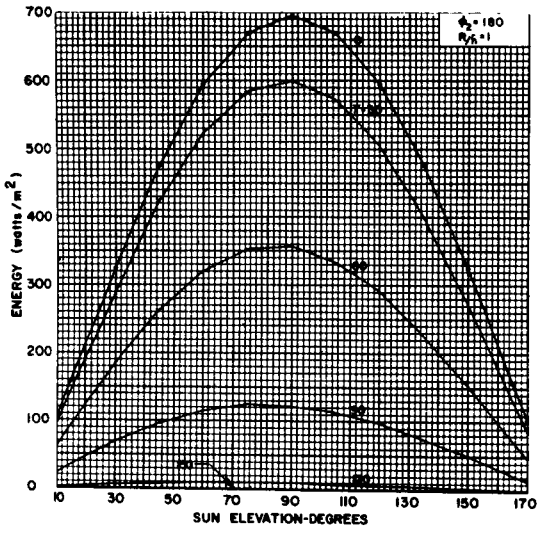

(d) $\phi_2 = 180°$, $R/\bar{h} = 1$

FIGURE 6. ENERGY INCIDENT ONTO ONE SIDE OF UNIT AREA (dA_2) VERSUS SUN ELEVATION ANGLE FOR VARIOUS ORIENTATIONS OF dA_2

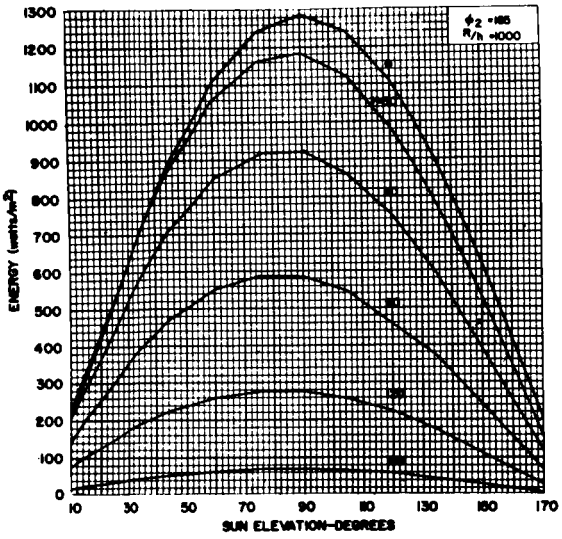

(a) $\phi_2 = 165°$, $R/\bar{h} = 1000$

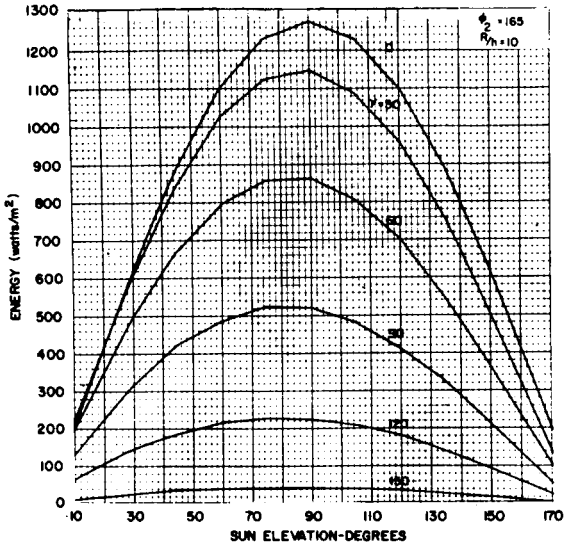

(b) $\phi_2 = 165°$, $R/\bar{h} = 10$

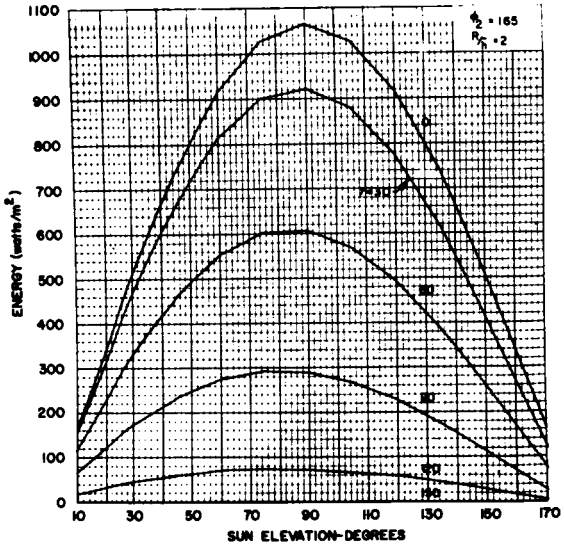

(c) $\phi_2 = 165°$, $R/\bar{h} = 2$

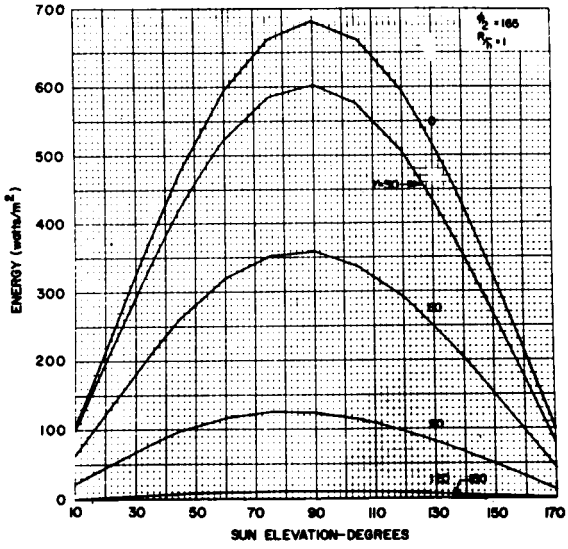

(d) $\phi_2 = 165°$, $R/\bar{h} = 1$

FIGURE 7. ENERGY INCIDENT ONTO ONE SIDE OF UNIT AREA (dA_2) VERSUS SUN ELEVATION ANGLE FOR VARIOUS ORIENTATIONS OF dA_2

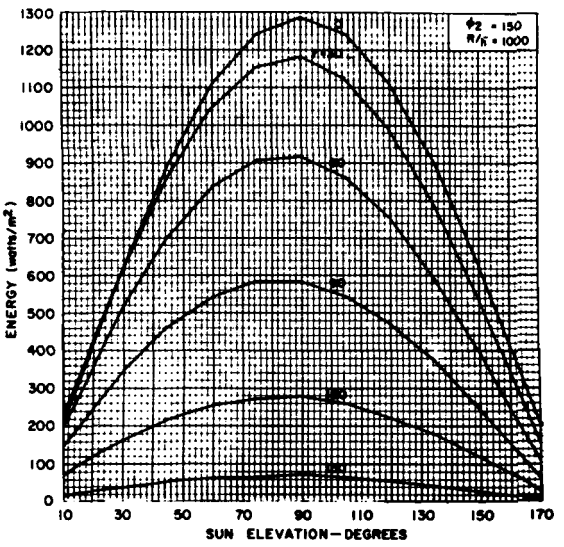

(a) $\phi_2 = 150°$, $R/\overline{h} = 1000$

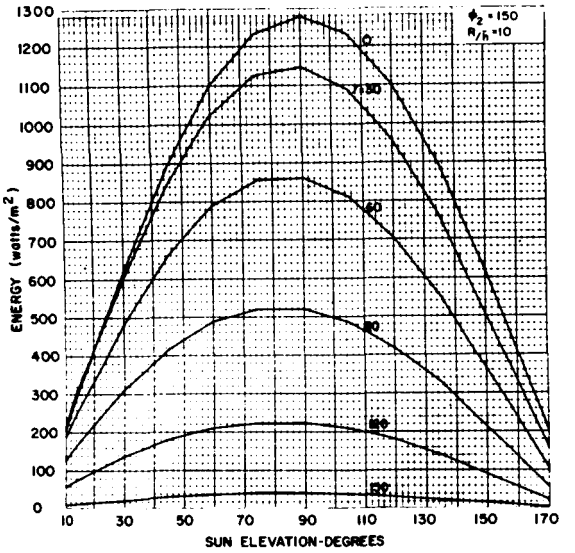

(b) $\phi_2 = 150°$, $R/\overline{h} = 10$

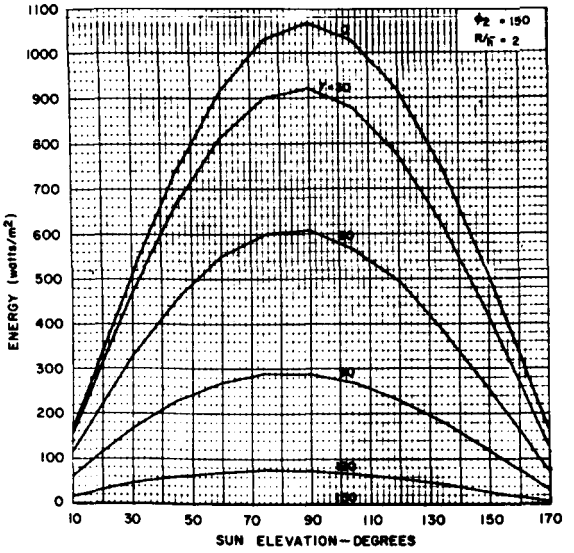

(c) $\phi_2 = 150°$, $R/\overline{h} = 2$

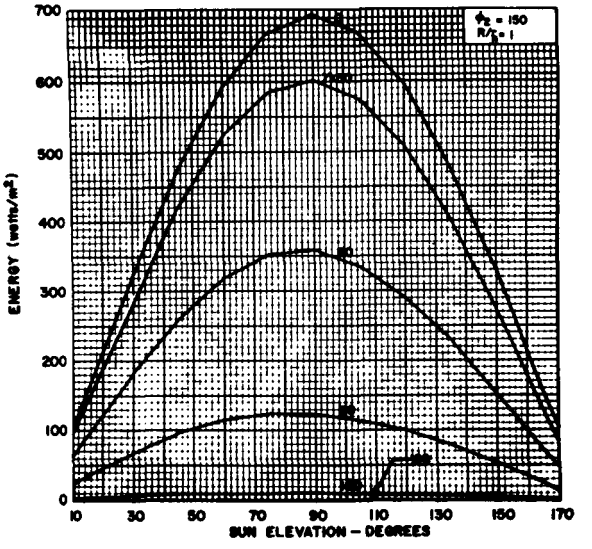

(d) $\phi_2 = 150°$, $R/\overline{h} = 1$

FIGURE 8. ENERGY INCIDENT ONTO ONE SIDE OF UNIT AREA (dA_2) VERSUS SUN ELEVATION ANGLE FOR VARIOUS ORIENTATIONS OF dA_2

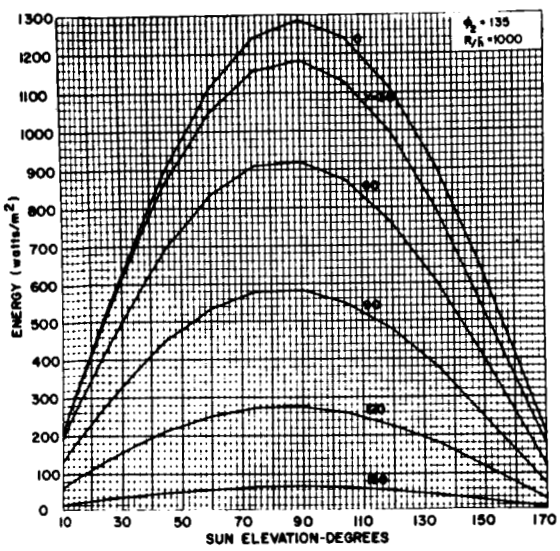

(a) $\phi_2 = 135°$, $R/\bar{h} = 1000$

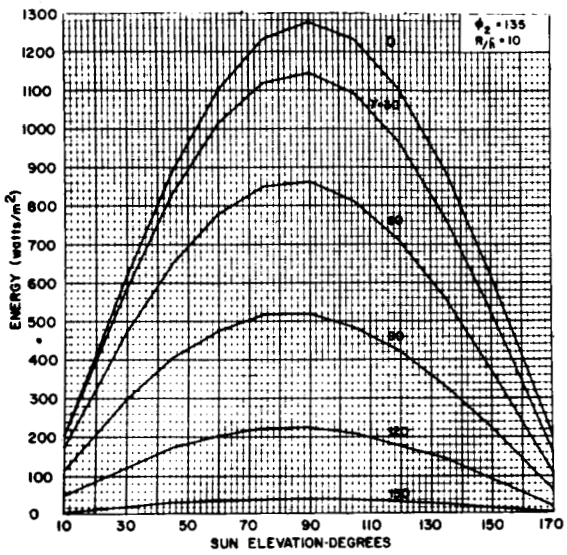

(b) $\phi_2 = 135°$, $R/\bar{h} = 10$

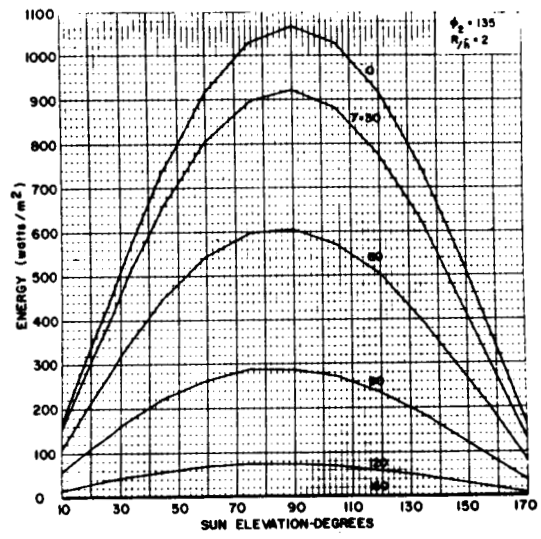

(c) $\phi_2 = 135°$, $R/\bar{h} = 2$

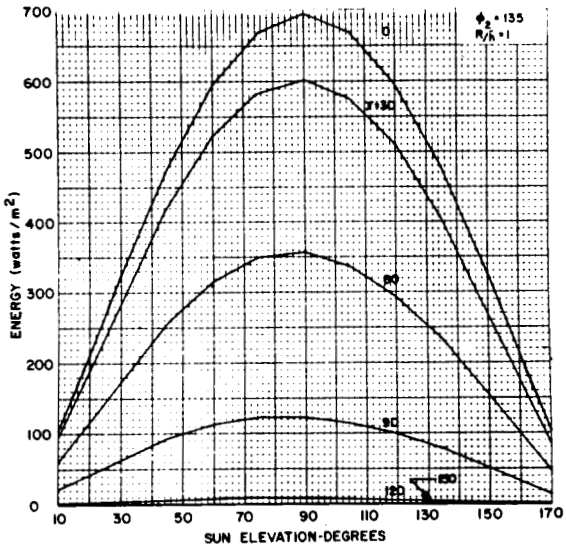

(d) $\phi_2 = 135°$, $R/\bar{h} = 1$

FIGURE 9. ENERGY INCIDENT ONTO ONE SIDE OF UNIT AREA (dA_2) VERSUS SUN ELEVATION ANGLE FOR VARIOUS ORIENTATIONS OF dA_2

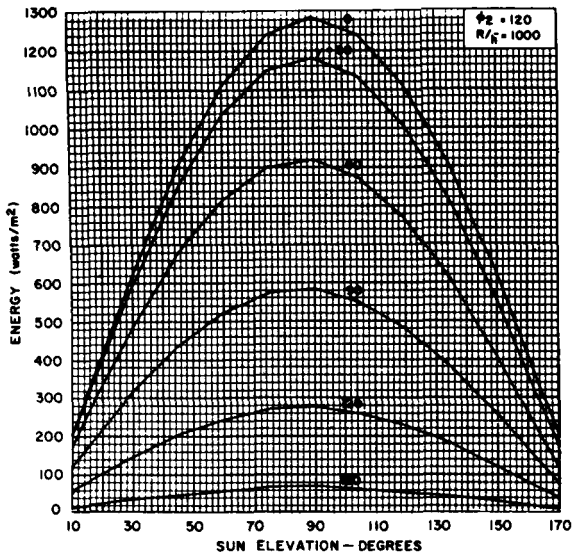

(a) $\phi_2 = 120°$, $R/\overline{h} = 1000$

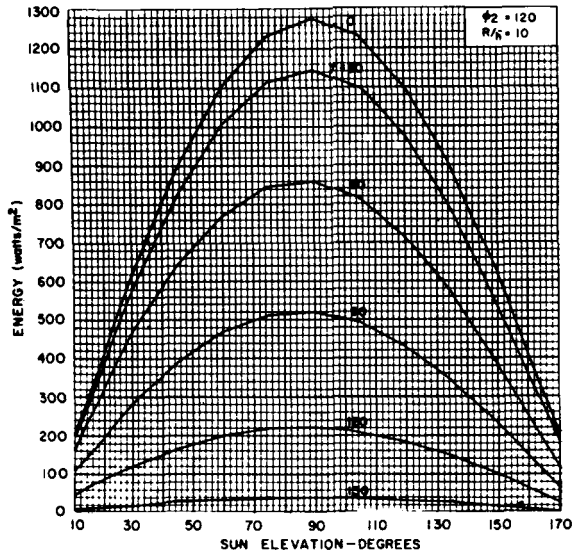

(b) $\phi_2 = 120°$, $R/\overline{h} = 10$

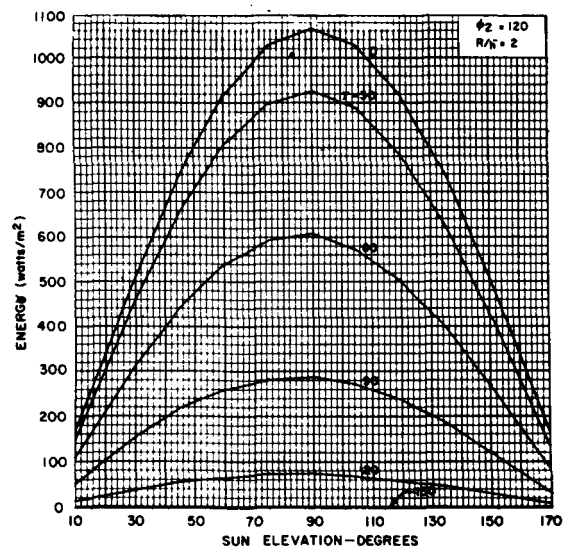

(c) $\phi_2 = 120°$, $R/\overline{h} = 2$

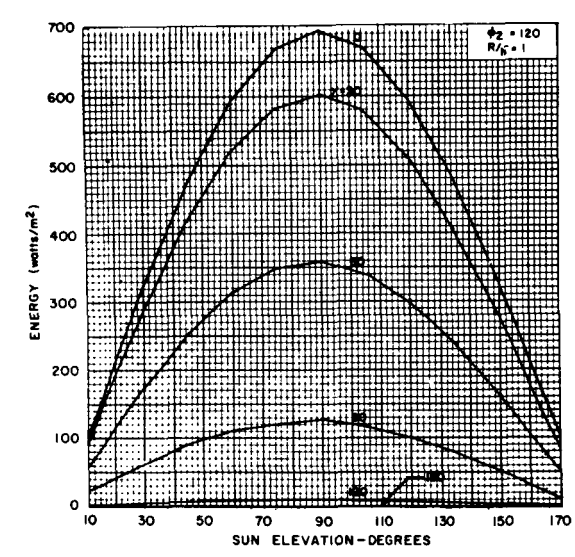

(d) $\phi_2 = 120°$, $R/\overline{h} = 1$

FIGURE 10. ENERGY INCIDENT ONTO ONE SIDE OF UNIT AREA (dA_2) VERSUS SUN ELEVATION ANGLE FOR VARIOUS ORIENTATIONS OF dA_2

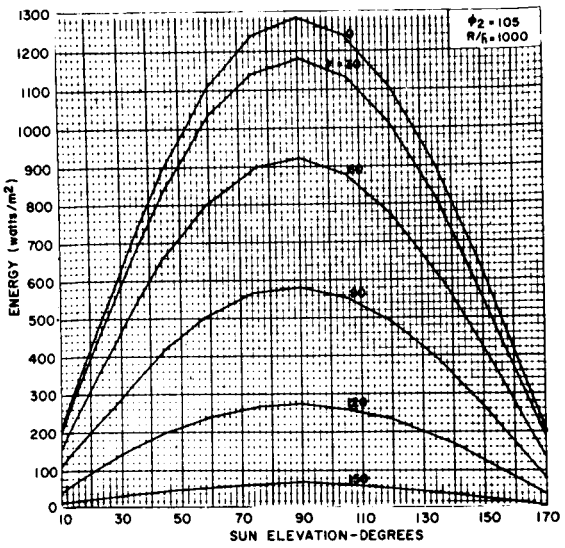

(a) $\phi_2 = 105°$, $R/\bar{h} = 1000$

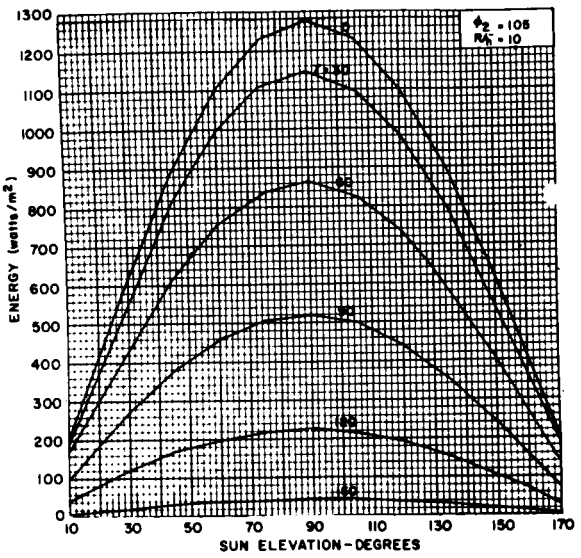

(b) $\phi_2 = 105°$, $R/\bar{h} = 10$

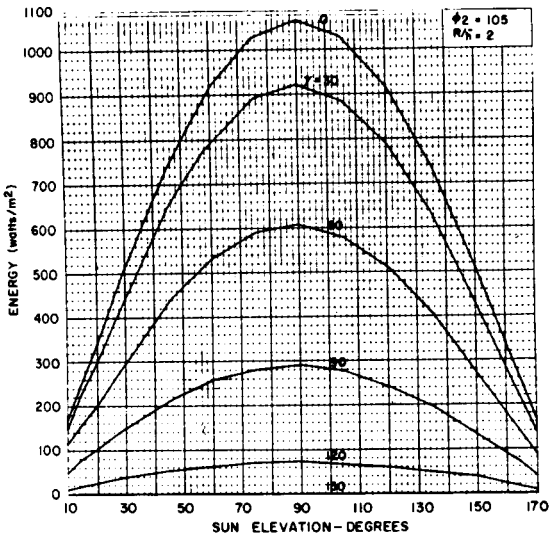

(c) $\phi_2 = 105°$, $R/\bar{h} = 2$

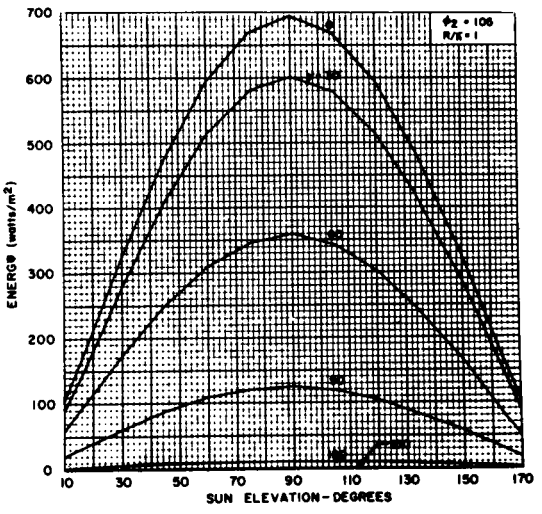

(d) $\phi_2 = 105°$, $R/\bar{h} = 1$

FIGURE 11. ENERGY INCIDENT ONTO ONE SIDE OF UNIT AREA (dA_2) VERSUS SUN ELEVATION ANGLE FOR VARIOUS ORIENTATIONS OF dA_2

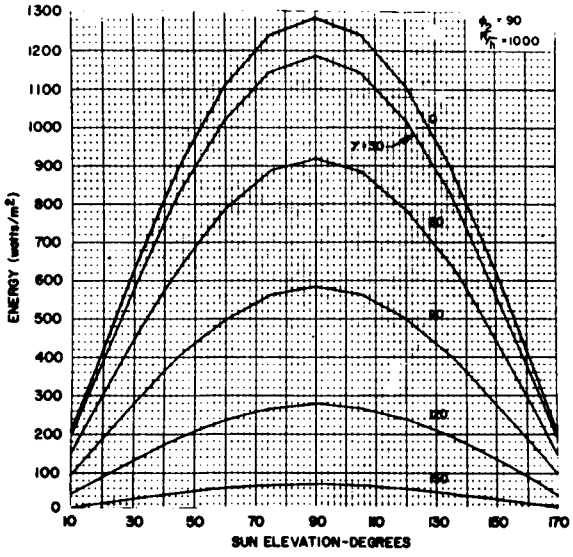

(a) $\phi_2 = 90°$, $R/\bar{h} = 1000$

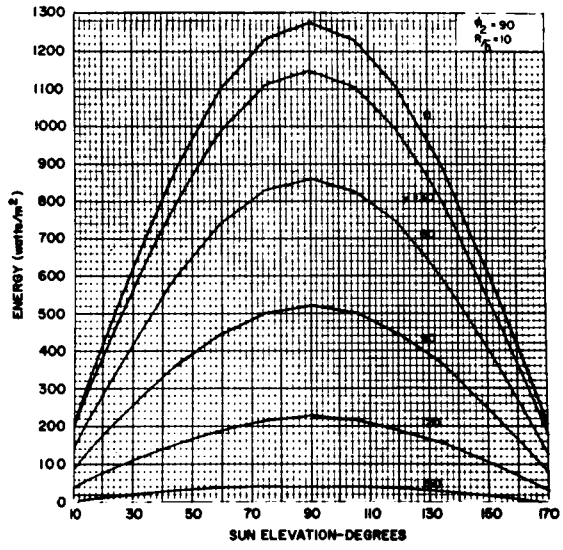

(b) $\phi_2 = 90°$, $R/\bar{h} = 10$

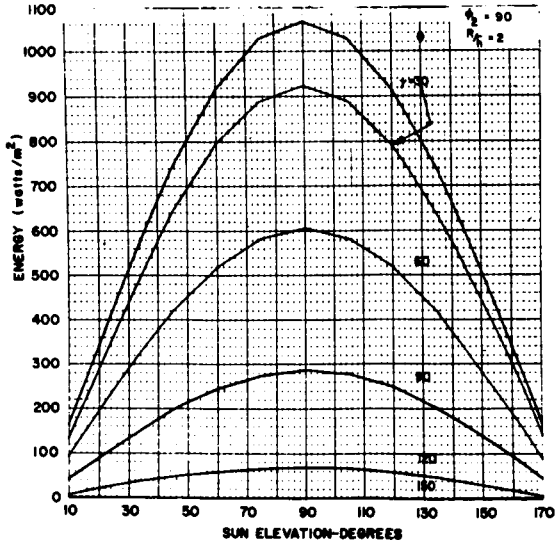

(c) $\phi_2 = 90°$, $R/\bar{h} = 2$

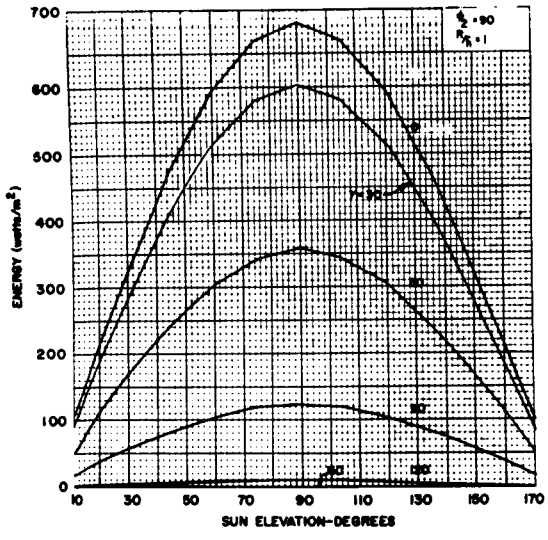

(d) $\phi_2 = 90°$, $R/\bar{h} = 1$

FIGURE 12. ENERGY INCIDENT ONTO ONE SIDE OF UNIT AREA (dA_2) VERSUS SUN ELEVATION ANGLE FOR VARIOUS ORIENTATIONS OF dA_2

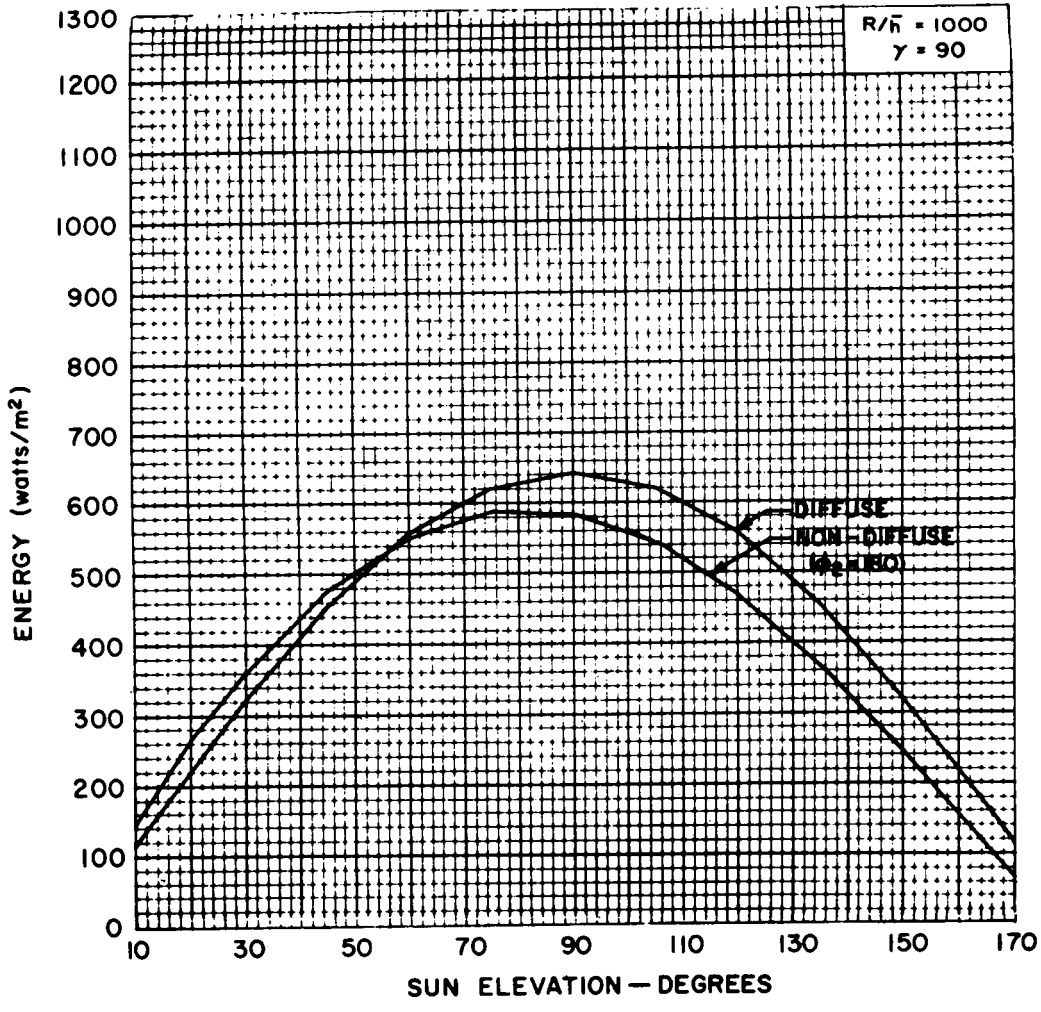

FIGURE 13. COMPARISON OF ENERGY INCIDENT ONTO dA_2 FOR DIFFUSE AND NON-DIFFUSE CASES

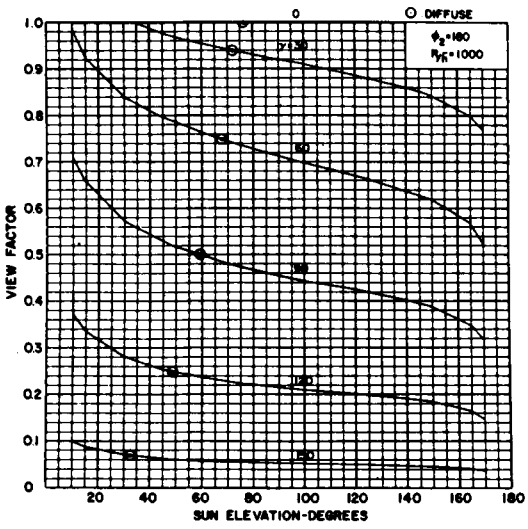

(a) $\phi_2 = 180°$, $R/\bar{h} = 1000$

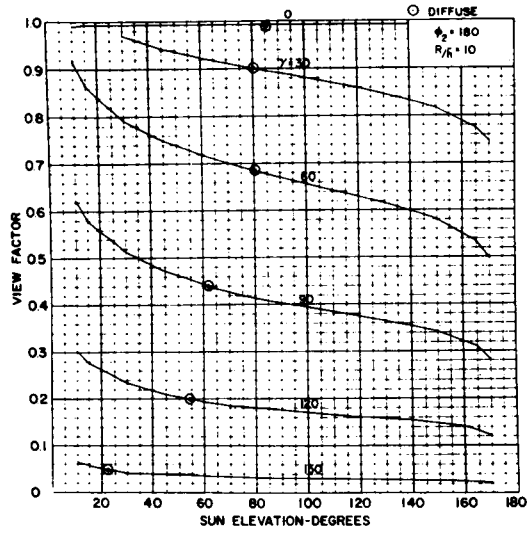

(b) $\phi_2 = 180°$, $R/\bar{h} = 10$

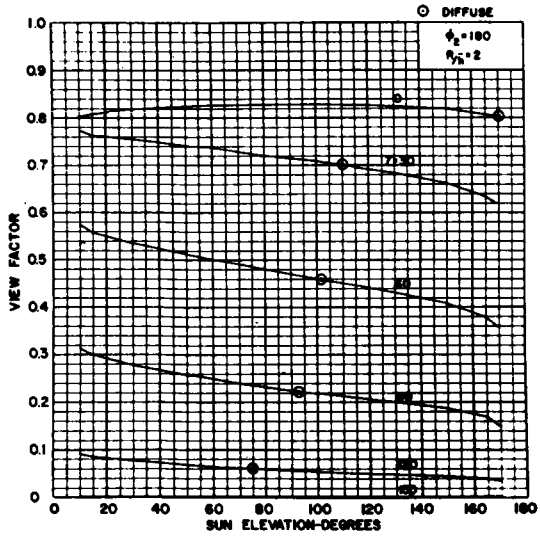

(c) $\phi_2 = 180°$, $R/\bar{h} = 2$

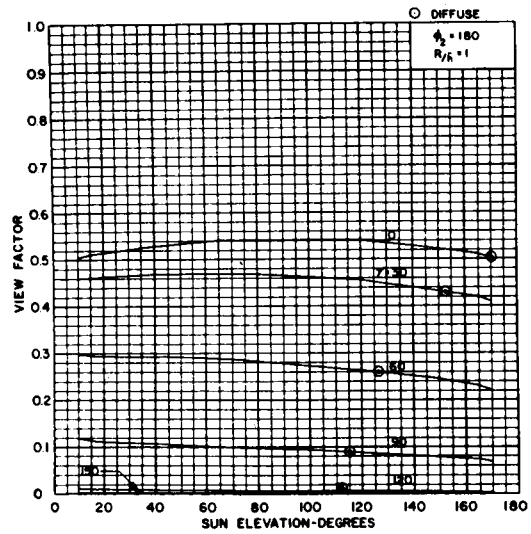

(d) $\phi_2 = 180°$, $R/\bar{h} = 1$

FIGURE 14. NORMALIZED ENERGY (VIEW FACTOR) FOR RADIATION BETWEEN LUNAR SURFACE AND ONE SIDE OF UNIT AREA (dA_2) VERSUS SUN ELEVATION ANGLE FOR VARIOUS ORIENTATIONS OF dA_2

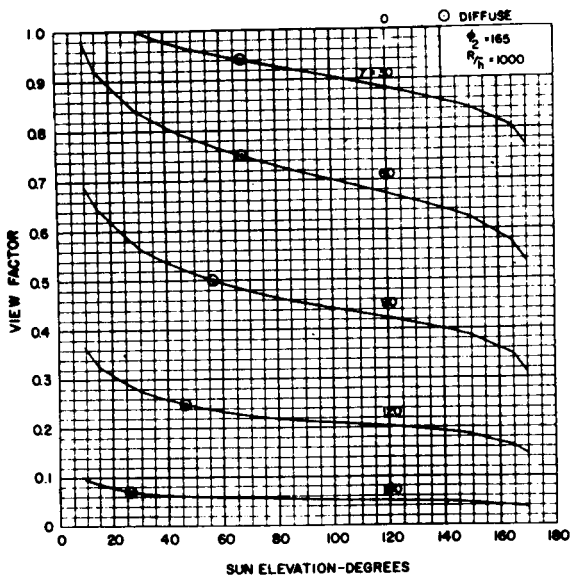

(a) $\phi_2 = 165°$, $R/\bar{h} = 1000$

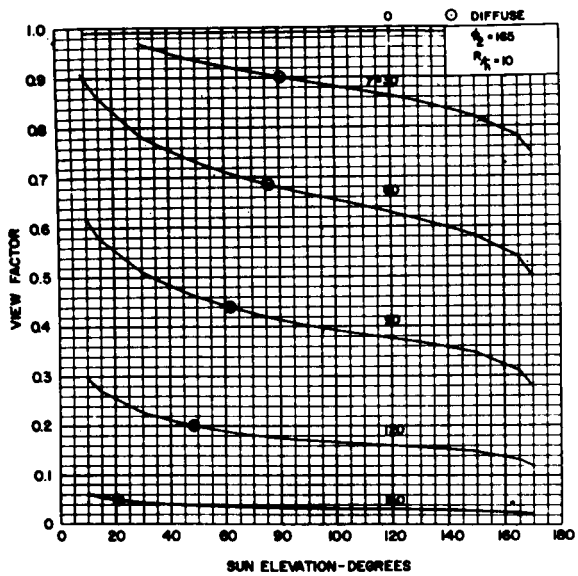

(b) $\phi_2 = 165°$, $R/\bar{h} = 10$

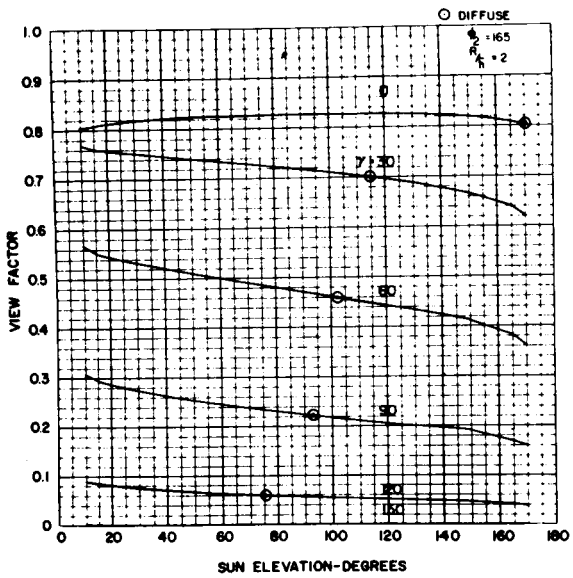

(c) $\phi_2 = 165°$, $R/\bar{h} = 2$

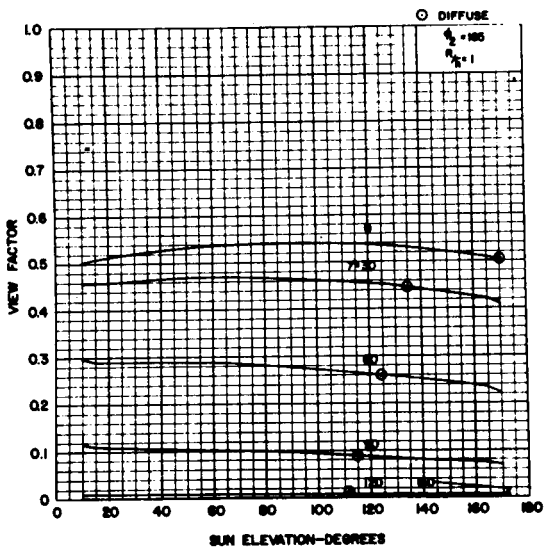

(d) $\phi_2 = 165°$, $R/\bar{h} = 1$

FIGURE 15. NORMALIZED ENERGY (VIEW FACTOR) FOR RADIATION BETWEEN LUNAR SURFACE AND ONE SIDE OF UNIT AREA (dA_2) VERSUS SUN ELEVATION ANGLE FOR VARIOUS ORIENTATIONS OF dA_2

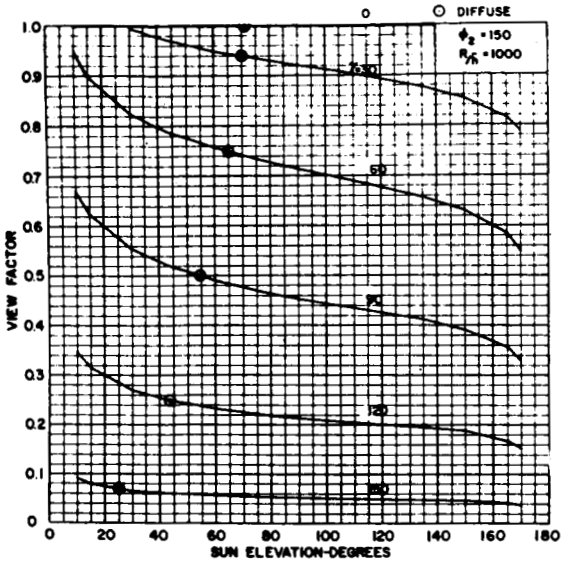

(a) $\phi_2 = 150°$, $R/\bar{h} = 1000$

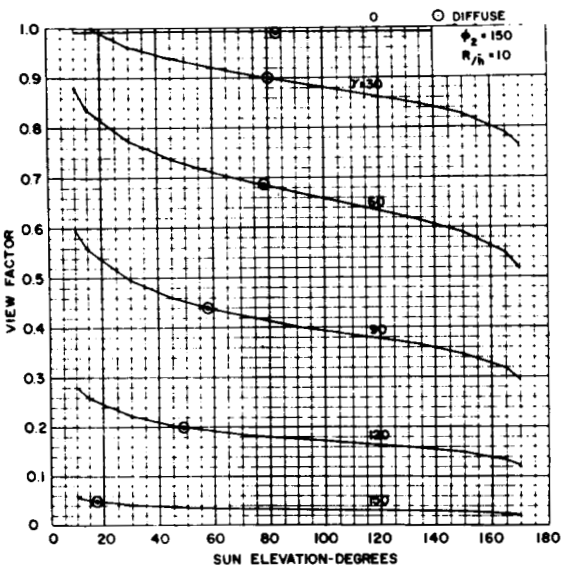

(b) $\phi_2 = 150°$, $R/\bar{h} = 10$

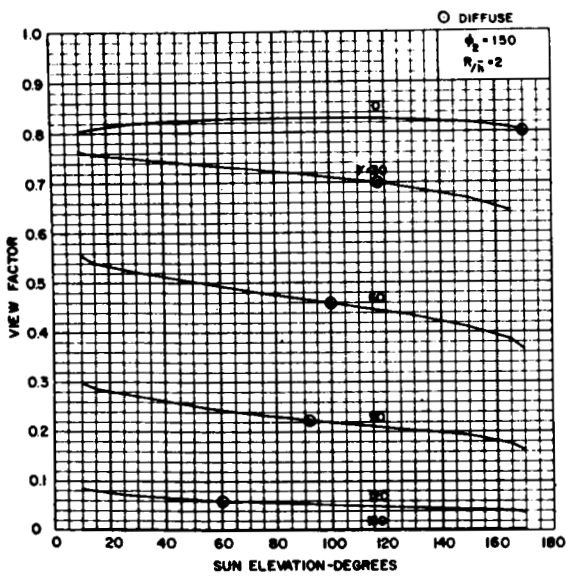

(c) $\phi_2 = 150°$, $R/\bar{h} = 2$

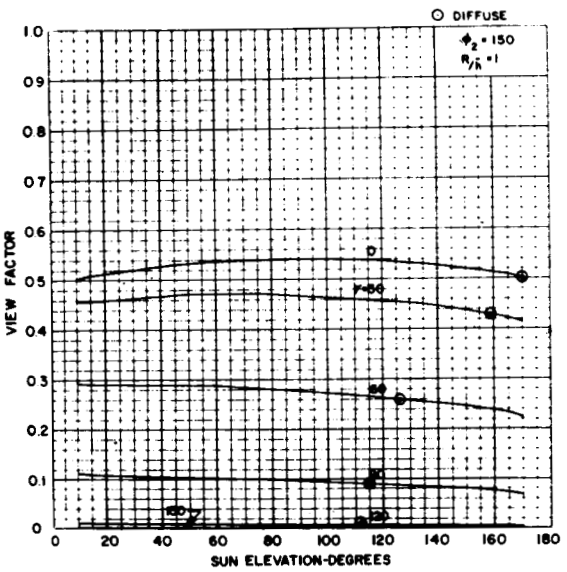

(d) $\phi_2 = 150°$, $R/\bar{h} = 1$

FIGURE 16. NORMALIZED ENERGY (VIEW FACTOR) FOR RADIATION BETWEEN LUNAR SURFACE AND ONE SIDE OF UNIT AREA (dA_2) VERSUS SUN ELEVATION ANGLE FOR VARIOUS ORIENTATIONS OF dA_2

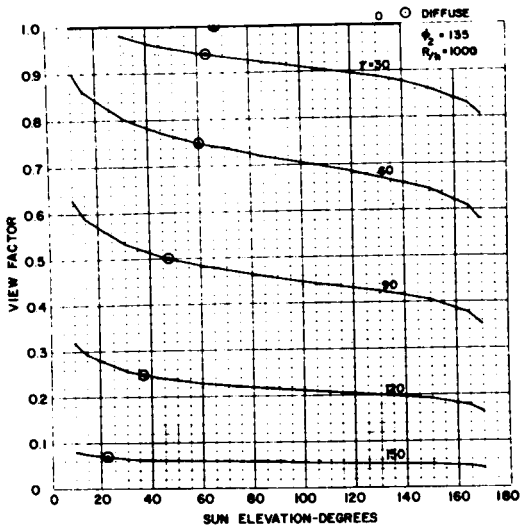

(a) $\phi_2 = 135°$, $R/\bar{h} = 1000$

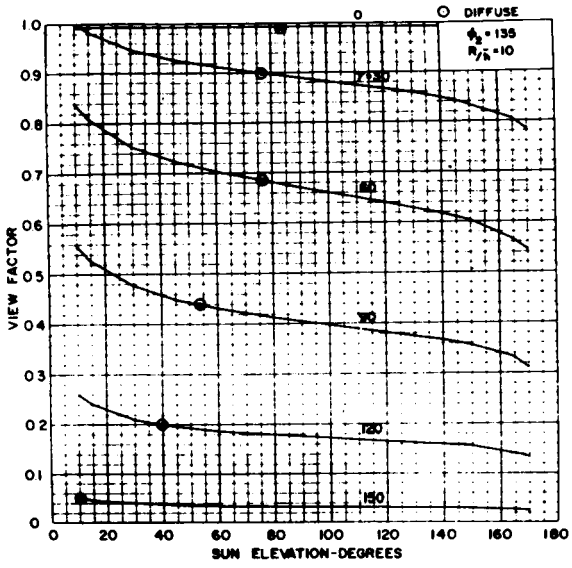

(b) $\phi_2 = 135°$, $R/\bar{h} = 10$

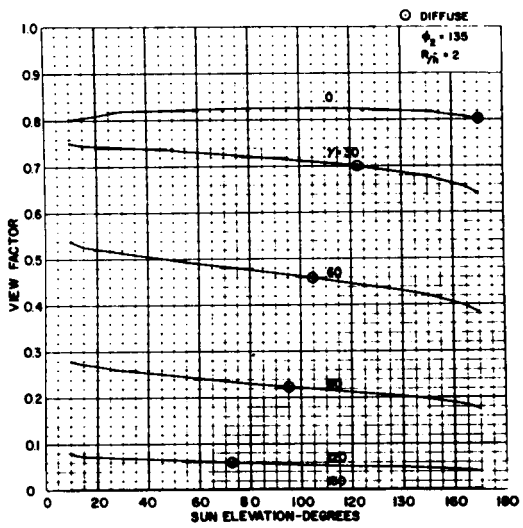

(c) $\phi_2 = 135°$, $R/\bar{h} = 2$

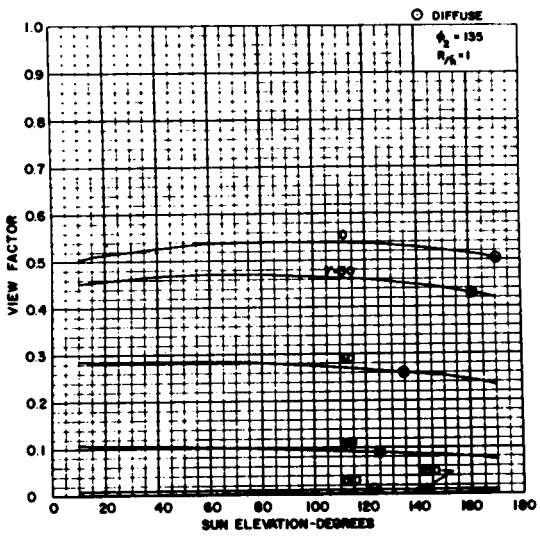

(d) $\phi_2 = 135°$, $R/\bar{h} = 1$

FIGURE 17. NORMALIZED ENERGY (VIEW FACTOR) FOR RADIATION BETWEEN LUNAR SURFACE AND ONE SIDE OF UNIT AREA (dA_2) VERSUS SUN ELEVATION ANGLE FOR VARIOUS ORIENTATIONS OF dA_2

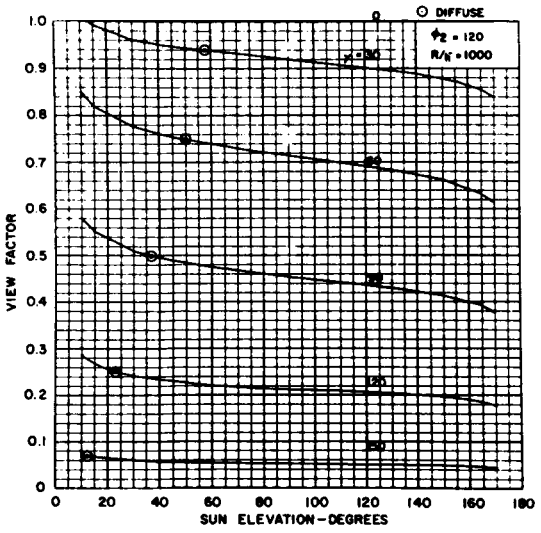

(a) $\phi_2 = 120°$, $R/\bar{h} = 1000$

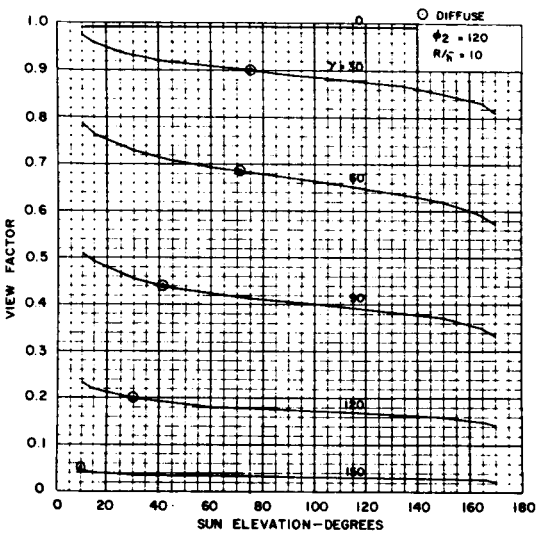

(b) $\phi_2 = 120°$, $R/\bar{h} = 10$

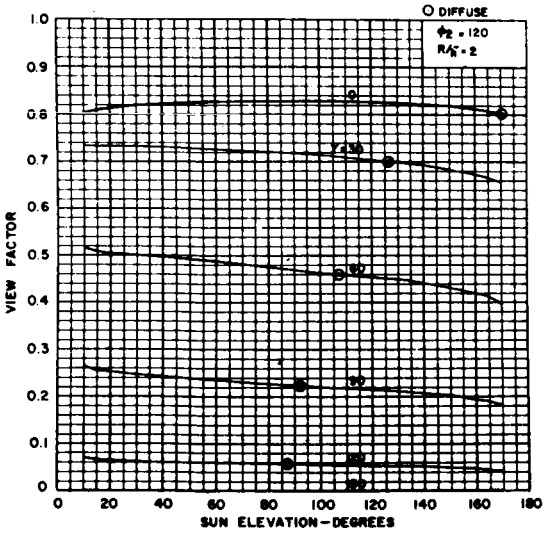

(c) $\phi_2 = 120°$, $R/\bar{h} = 2$

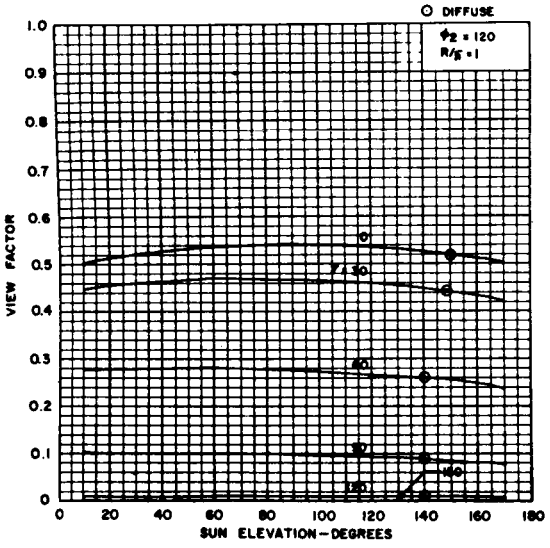

(d) $\phi_2 = 120°$, $R/\bar{h} = 1$

FIGURE 18. NORMALIZED ENERGY (VIEW FACTOR) FOR RADIATION BETWEEN LUNAR SURFACE AND ONE SIDE OF UNIT AREA (dA_2) VERSUS SUN ELEVATION ANGLE FOR VARIOUS ORIENTATIONS OF dA_2

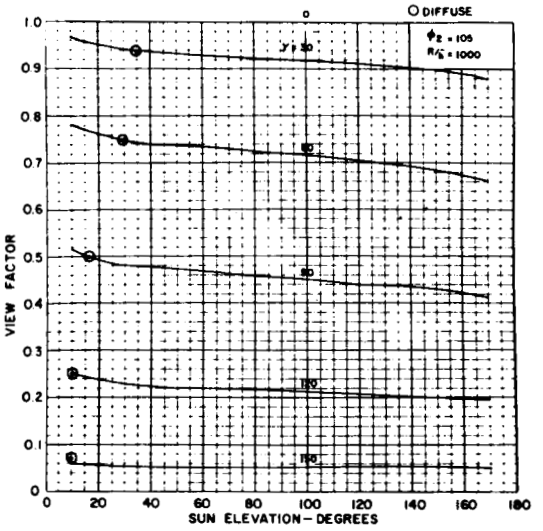

(a) $\phi_2 = 105°$, $R/\bar{h} = 1000$

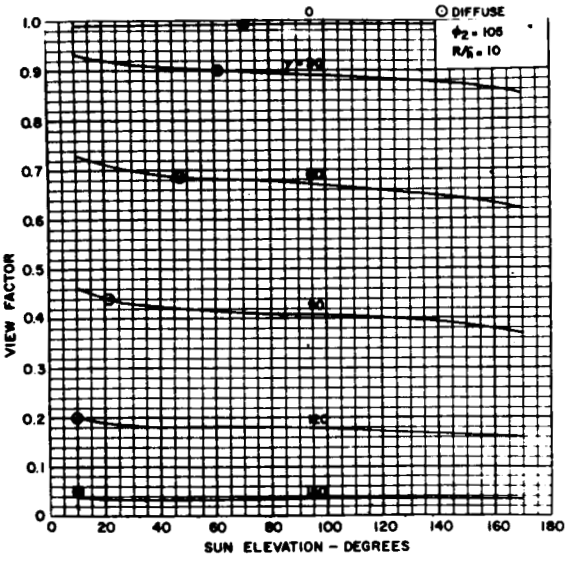

(b) $\phi_2 = 105°$, $R/\bar{h} = 10$

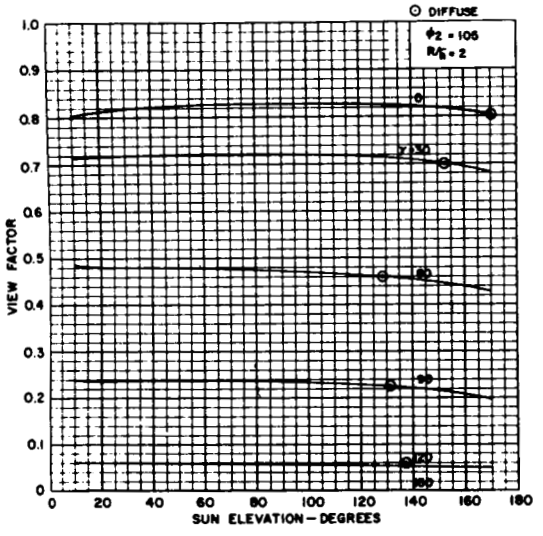

(c) $\phi_2 = 105°$, $R/\bar{h} = 2$

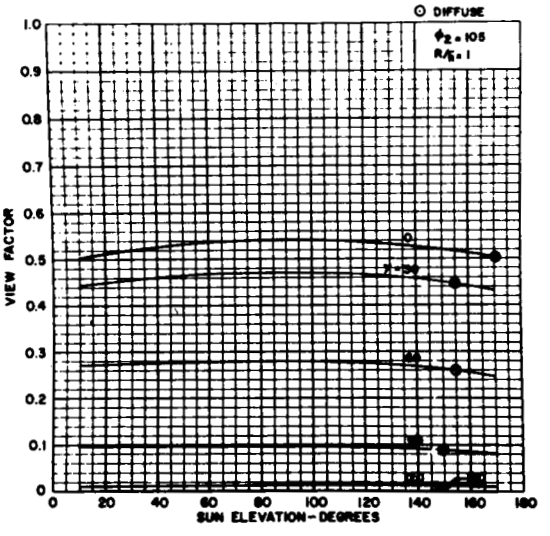

(d) $\phi_2 = 105°$, $R/\bar{h} = 1$

FIGURE 19. NORMALIZED ENERGY (VIEW FACTOR) FOR RADIATION BETWEEN LUNAR SURFACE AND ONE SIDE OF UNIT AREA (dA_2) VERSUS SUN ELEVATION ANGLE FOR VARIOUS ORIENTATIONS OF dA_2

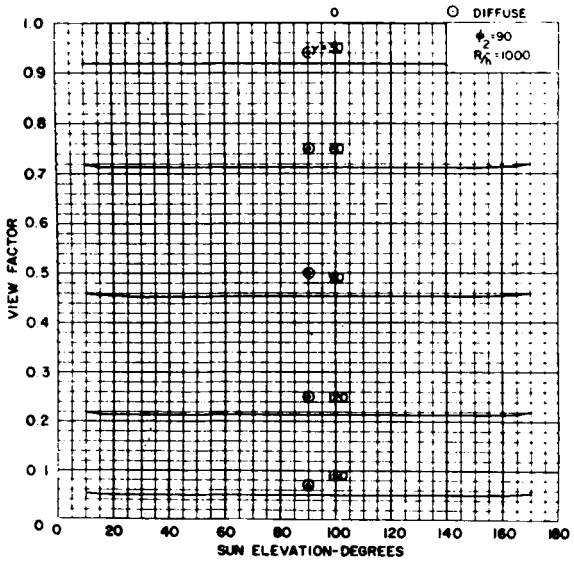

(a) $\phi_2 = 90°$, $R/\bar{h} = 1000$

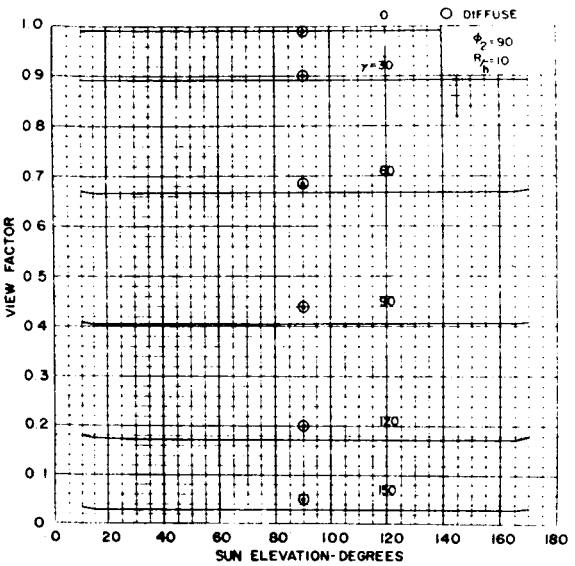

(b) $\phi_2 = 90°$, $R/\bar{h} = 10$

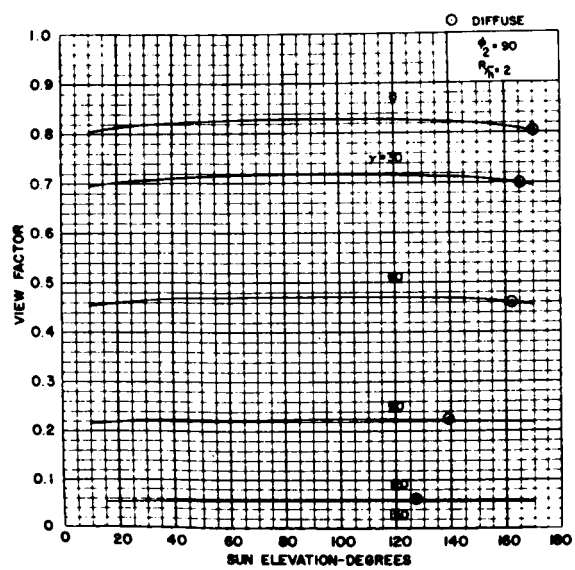

(c) $\phi_2 = 90°$, $R/\bar{h} = 2$

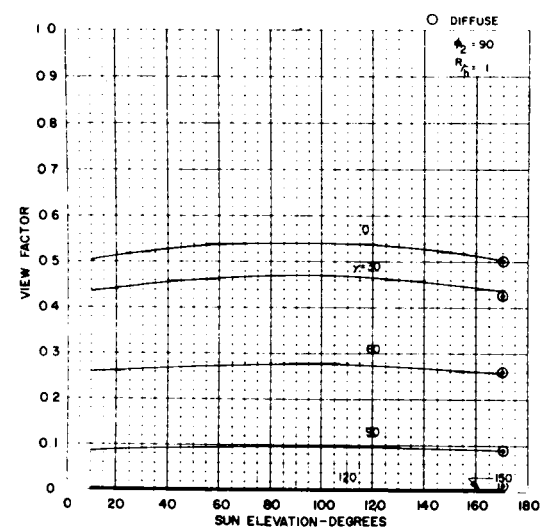

(d) $\phi_2 = 90°$, $R/\bar{h} = 1$

FIGURE 20. NORMALIZED ENERGY (VIEW FACTOR) FOR RADIATION BETWEEN LUNAR SURFACE AND ONE SIDE OF UNIT AREA (dA_2) VERSUS SUN ELEVATION ANGLE FOR VARIOUS ORIENTATIONS OF dA_2

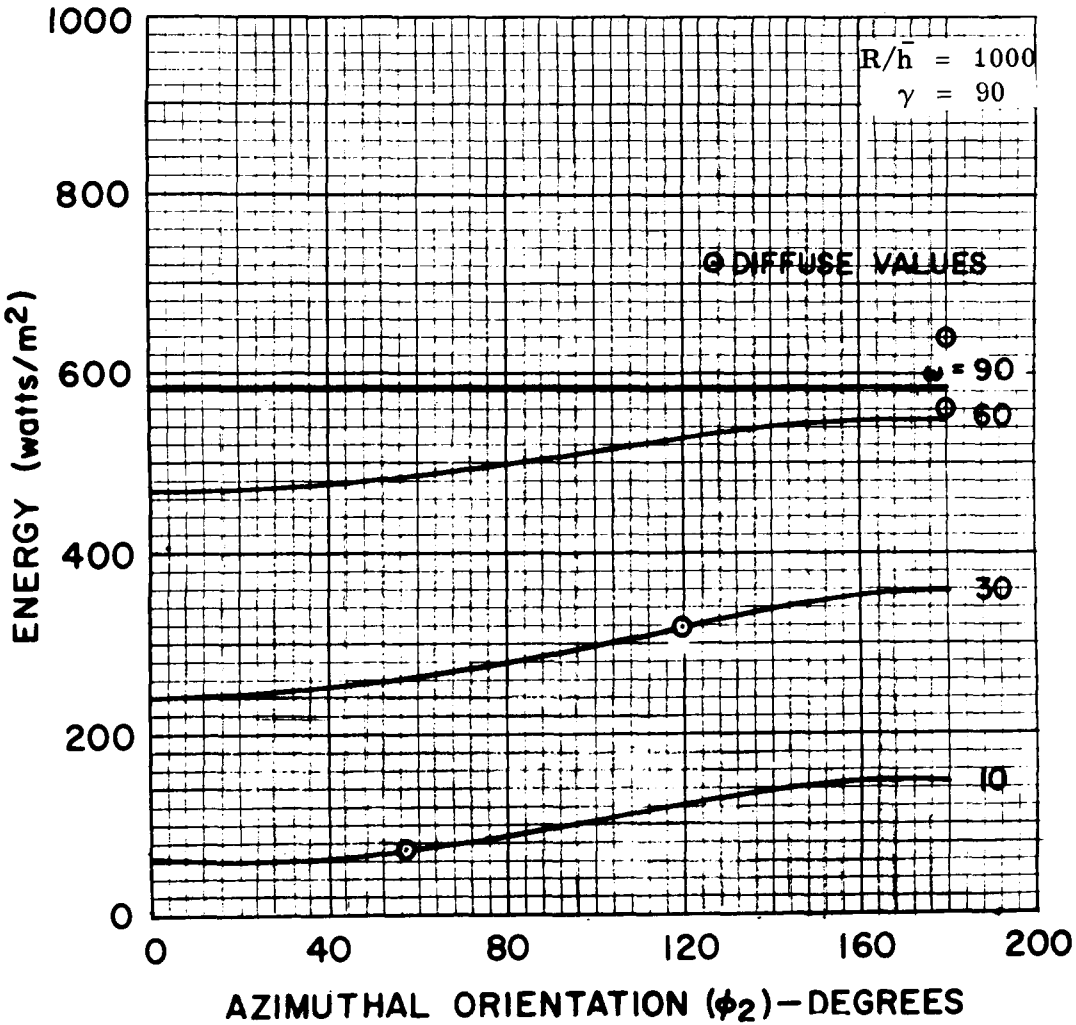

FIGURE 21. ENERGY INCIDENT ONTO dA_2 WHILE ROTATING dA_2 ABOUT THE Z AXIS FOR VARIOUS SUN ELEVATIONS (ω)

"The aeronautical and space activities of the United States shall be conducted so as to contribute . . . to the expansion of human knowledge of phenomena in the atmosphere and space. The Administration shall provide for the widest practicable and appropriate dissemination of information concerning its activities and the results thereof."

—NATIONAL AERONAUTICS AND SPACE ACT OF 1958

NASA SCIENTIFIC AND TECHNICAL PUBLICATIONS

TECHNICAL REPORTS: Scientific and technical information considered important, complete, and a lasting contribution to existing knowledge.

TECHNICAL NOTES: Information less broad in scope but nevertheless of importance as a contribution to existing knowledge.

TECHNICAL MEMORANDUMS: Information receiving limited distribution because of preliminary data, security classification, or other reasons.

CONTRACTOR REPORTS: Scientific and technical information generated under a NASA contract or grant and considered an important contribution to existing knowledge.

TECHNICAL TRANSLATIONS: Information published in a foreign language considered to merit NASA distribution in English.

SPECIAL PUBLICATIONS: Information derived from or of value to NASA activities. Publications include conference proceedings, monographs, data compilations, handbooks, sourcebooks, and special bibliographies.

TECHNOLOGY UTILIZATION PUBLICATIONS: Information on technology used by NASA that may be of particular interest in commercial and other non-aerospace applications. Publications include Tech Briefs, Technology Utilization Reports and Notes, and Technology Surveys.

Details on the availability of these publications may be obtained from:

SCIENTIFIC AND TECHNICAL INFORMATION DIVISION

NATIONAL AERONAUTICS AND SPACE ADMINISTRATION

Washington, D.C. 20546